

**North east Pacific Time-series Underwater Networked
Experiment (NEPTUNE):
Power System Design, Modeling and Analysis**

Aditya Upadhye

A thesis submitted in partial fulfillment of the requirements for the degree of

Master of Science in Electrical Engineering

University of Washington

2003

Program Authorized to Offer Degree: Electrical Engineering

University of Washington

Graduate School

This is to certify that I have examined this copy of a master's thesis by

Aditya Upadhye

and found that it is complete and satisfactory in all respects,
and that any and all revisions required by the final
examining committee have been made.

Committee Members:

Mohamed A. El-Sharkawi

Robert J. Marks II

Bruce M. Howe

Date: _____

In presenting this thesis in partial fulfillment of the requirements for a Master's degree at the University of Washington, I agree that the Library shall make its copies freely available for inspection. I further agree that extensive copying of this thesis is allowable only for scholarly purposes, consistent with "fair use" as prescribed in the U.S. Copyright Law. Any other reproduction for any purposes or by any means shall not be allowed without my written permission.

Signature: _____

Date: _____

Table of Contents

	Page
List of Figures	iii
List of Tables	vi
Chapter 1. Introduction.....	1
1.1 NEPTUNE General Introduction.....	1
1.2 NEPTUNE Power: Basic Concepts	2
1.3 Electromagnetic Transients Analyses	4
1.4 Switching and Sectionalization: Comparison of the Two Design Concepts	5
Chapter 2. Version 1 Design of the NEPTUNE Power System.....	9
2.1 Introduction.....	9
2.2 Design of the DC Circuit Breaker	12
2.3 Hardware Development of the DC Circuit Breaker Prototype	18
Chapter 3. Version 2 Design of the NEPTUNE Power System.....	25
3.1 Branching Unit Circuit Description.....	25
3.2 Modes of System Operation	27
3.3 Algorithms for Branching Unit Controller	32
Chapter 4. Electromagnetic Transients Analyses	37
4.1 Introduction.....	37
4.2 Dynamics of the NEPTUNE Power System.....	38
4.3 Electromagnetic Transients Program (EMTP)	40

Chapter 5.	Cable Analysis and Modeling.....	46
5.1	Introduction.....	46
5.2	Theoretical Calculation of Cable Inductance	46
5.3	Calculation of Capacitance	53
5.4	Computation of Cable Parameters by ATP	54
5.5	Computation of Ground Parameters	56
Chapter 6.	EMTP Models for Restrikes and Shore Station Control	59
6.1	Introduction.....	59
6.2	Initial Switching Arcs	60
6.3	Restrikes	61
6.4	Modeling of Shore Station Power Supply Controls	69
Chapter 7.	Network Transient Simulations	74
7.1	Introduction.....	74
7.2	Version 1: Simulation of Non-Fault System Operation	74
7.3	Version 1: Simulation of Fault Condition	81
7.4	Version 2: Fault Transient Studies	84
Chapter 8.	Conclusions and Future Work	91
	Future Work	92
	List of References	93

List of Figures

	Page
Figure 1.1 NEPTUNE cable system with approximate node locations	2
Figure 1.2 Version 1 and Version 2 power system designs	6
Figure 2.1 Structure of the NEPTUNE power system.....	9
Figure 2.2 Block schematic for science node	11
Figure 2.3 Conceptual schematic of the NEPTUNE node connected to backbone	13
Figure 2.4 Components of dc circuit breaker.....	14
Figure 2.5 CB soft closing	15
Figure 2.6 CB when fully closed	16
Figure 2.7 CB capacitor charging	17
Figure 2.8 CB capacitor discharging	17
Figure 2.9 Circuit diagram for driver circuit.....	21
Figure 2.10 Circuit diagram for TTL control logic.....	23
Figure 3.1 Branching unit circuit diagram.....	25
Figure 3.2 Zener series power supply	27
Figure 3.3 Overall system control actions	31
Figure 3.4 Typical setup in fault-locating mode.....	33
Figure 3.5 Steps in fault-locating mode.....	35
Figure 3.6 Steps in restoration mode	36
Figure 4.1 Switching in RL series circuit	37

Figure 4.2 Node locations and relative distances in km	39
Figure 4.3 Interface between network and TACS solution [3].....	45
Figure 5.1 Cross-section of tubular conductor.....	47
Figure 5.2 Proposed cable for the NEPTUNE observatory	50
Figure 6.1 Restrikes in a circuit breaker	62
Figure 6.2 Simulation circuit for restrike model.....	64
Figure 6.3 Current through capacitor with restrikes when $C=4\mu\text{F}$	66
Figure 6.4 Voltage across capacitor for $C=4\mu\text{F}$	66
Figure 6.5 Capacitor current without restrikes when $C=5\mu\text{F}$	67
Figure 6.6 Voltage across capacitor for $C=5\mu\text{F}$	68
Figure 6.7 Simulation circuit for shore station current limiting model	71
Figure 6.8 Output current of shore power supply during current limiting.....	72
Figure 6.9 Output voltage of shore power supply during current limiting	72
Figure 6.10 Output current of shore power supply without current limiting	73
Figure 7.1 Steady-state simulation circuit	75
Figure 7.2 Time sequence of node breaker switching	75
Figure 7.3 Current at the left input of Node 3.....	77
Figure 7.4 Voltage at the left input of Node 3	77
Figure 7.5 Voltage across the left diode on Node N3.....	78
Figure 7.6 Current through the left diode of Node N3	79
Figure 7.7 Voltage across the right diode of Node N3	79
Figure 7.8 Current through right diode of Node N3	80

Figure 7.9 Simulation of fault condition.....	81
Figure 7.10 Current entering Node 2	82
Figure 7.11 Voltage across Load Z2	82
Figure 7.12 Current flowing in fault	83
Figure 7.13 Capacitor current for node N2.....	84
Figure 7.14 Simulation circuit for study of pre-insertion resistance placement	86
Figure 7.15 Plot of fault energy against response time.....	88
Figure 7.16 Plot of peak transient current against the fault distance 'X'	89
Figure 7.17 Plot of fault energy against the fault distance 'X'	89

List of Tables

	Page
Table 1-1 Comparison of Version 1 and Version 2 power system designs	8
Table 2-1 Logic for switch operation in circuit breaker	22
Table 5-1 Comparison of cable parameter values.....	56
Table 5-2 Comparison of ground parameter values.....	58
Table 6-1 Restrike studies.....	65

Acknowledgements

This research is sponsored by the National Science Foundation through the grant titled, “Development of a Power System for Cabled Ocean Observatories.” The author wishes to express sincere appreciation to the sponsors. The author also wishes to thank the NEPTUNE Power Group, especially Dr. Harold Kirkham of Jet Propulsion Laboratory, Dr. Bruce Howe of Applied Physics Laboratory and Professor Chen-Ching Liu for their insightful inputs. The author thanks the members of Computational Intelligence Applications Laboratory for their constant encouragement, especially Professor Mohamed El-Sharkawi for his patience, support and guidance.

Chapter 1. Introduction

1.1 NEPTUNE General Introduction

The vast oceans of the world have not yet been explored completely. Current technology allows autonomous vehicles or remotely operated vehicles (ROVs) to go to the deep ocean floor to carry out scientific experiments. ROV operations are based on ships; mission control and monitoring is from these ships. To carry out science experiments in the ocean for an extended time, technology beyond ROVs and similar equipment is required. A permanent observatory can be used as a base for various scientific fields to explore the ocean and its various features.

The NEPTUNE project plans to deploy a fiber-optic/power cable network around and across the Juan de Fuca tectonic plate off the west coast of North America. NEPTUNE will study a variety of geological, oceanographic and ecological processes.

It is envisioned that the NEPTUNE backbone will be comprised of 3000 km of cable connecting about 30-40 evenly distributed nodes (Figure 1.1). Branch cables will be used to extend the network to any location on the plate. Each node will provide standard power and Internet communication interfaces for experimentation. The complete network will carry about 10 gigabits per second of data, and deliver 200 kW of power with an operational life span of at least 30 years [1].

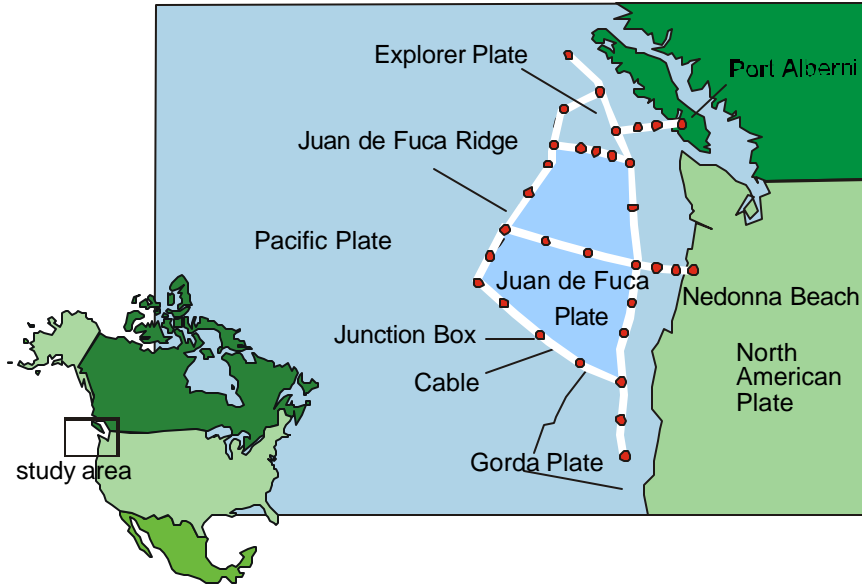


Figure 1.1 NEPTUNE cable system with approximate node locations

1.2 NEPTUNE Power: Basic Concepts

The NEPTUNE power system is required to satisfy the power requirements of all scientific equipments at all nodes. This power is to be delivered by conventional submarine telecommunications cable used in many sub-sea telecom systems all over the world. The design of the cable is to serve a dual purpose; it has a hollow core to carry fiber optics and the sheath of the cable (copper) carries the load current. A detailed discussion on the cable used and its analysis is included in Chapter 5. The power delivery system is operated as an interconnected network in order to maximize both reliability and power level. The cable is energized by dc in order to reduce complexity of design and cost. The ocean provides the return path for the current. At each node, a dc-dc converter will reduce the incoming supply from about 10kV to 400V.

1.2.1 Basic tradeoffs

In the NEPTUNE power system design, a few basic tradeoffs are studied [2].

1.2.1.1 Frequency of operation; ac versus dc.

If ac power were used, the charging current of the capacitance would be large and continuous because the capacitance of the NEPTUNE cable is large. Adding shunt inductors would compensate this but add to the overall cost. Using dc power eliminates this cost. Very low frequency (0.1 Hz) could be used, but the low frequency ac would add unjustifiable complexity at the nodes where ac-dc conversion will be needed.

1.2.1.2 Structure of the network; interconnected versus radial.

In terrestrial power systems, apart from the distribution systems, which are radial, the network is interconnected. This has made the terrestrial power delivery system generally robust. The cascading effect of faults that can sometimes occur in terrestrial systems is prevented by load shedding. This principle can be used for NEPTUNE and the reliability that is gained by an interconnected network is considerable.

1.2.1.3 Connection of loads; series versus parallel.

A parallel scheme of load serving has been chosen for NEPTUNE, based on the fact that the NEPTUNE network is intended to be interconnected and a parallel scheme is able to transmit more power compared to a series scheme.

1.3 Electromagnetic Transients Analyses

In conventional terrestrial power systems switching actions, short-circuits, lightning strikes, and disturbances during normal operation often cause temporary overvoltages and high frequency current oscillations. The power system should be capable of withstanding these overvoltages without any damage to system components. The simulation of these transient voltages and currents is significant for the design of system components, analysis of various possible operating conditions and the proper functioning of the system protection. Transients are usually composed of traveling waves on high voltage transmission lines or underground cables or oscillations in network elements such as generators and transformers.

The NEPTUNE power system is a large-scale, 10 kV dc network of cables, power supplies, circuit breakers, converters, loads and control equipment. Because of the highly reactive nature of NEPTUNE cables and the need to interrupt the dc currents in the backbone system as well as the branches, it is important to perform transient analyses of the system to identify excessive overvoltages, overcurrents and high frequency transients. These analyses help design the various components of the circuit breaker and verify the robustness of the system.

The selected transient simulator for project NEPTUNE is the Alternative Transients Program (ATP). The ATP is based on the Electromagnetic Transient Program (EMTP) used by the power industry for transient simulations. The ATP has extensive modeling capabilities for lines, cables, breakers, loads, converters, protection devices, non-linear elements, electromagnetic coupling, and major power electronics devices and equipment. The ATP has an enhanced graphical interface called ATPDraw that allows easy entry of system topology and data. The functions and working of ATP is described in detail in [3].

1.4 Switching and Sectionalization: Comparison of the Two Design Concepts

The cable sections in the NEPTUNE network must be isolated from the rest of the system in certain operating scenarios. Normally this function is performed by the circuit breakers capable of interrupting fault current, and isolators capable only of interrupting load current.

Because there are no naturally occurring current zeroes, direct current is non-trivial to interrupt. This is particularly true of the problem of interrupting faults in the NEPTUNE system, where the current available from the discharge of the cable capacitance can be large and sustained. The approach normally taken to implement a DC breaker is to force a current zero by diverting the electrical energy to a storage device, e.g.: a capacitor. This approach is the one taken in the *Version 1* design of the NEPTUNE power system. Details of this approach are included in Chapter 2.

Another approach for sectionalizing the NEPTUNE network follows the philosophy that faults in submarine cables are rare and de-energization of the entire system will be needed only a few times over the entire lifetime of the project. Emphasis is given to increasing the reliability of the system. Thus the system can be de-energized before performing the switching. This approach allows the switching to take place without any possibility of arcing and restrikes, as the current interrupted is very small. The *Version 2* design of the NEPTUNE Power System takes this approach and is described in Chapter 3.

Figure 1.2 shows the general schematic of the two versions. In Version 1 the node contains the switches along with the dc-dc converter and the control circuitry. The power is delivered to the node using a two-conductor spur cable. Version 1 contains a *passive* branching unit, which contains no switching elements. In Version 2, the dc-dc converter and other control circuitry is located in the science node, fed from the backbone via a

single conductor spur cable. A separate *active* branching unit houses the sectionalizing switch and its controls.

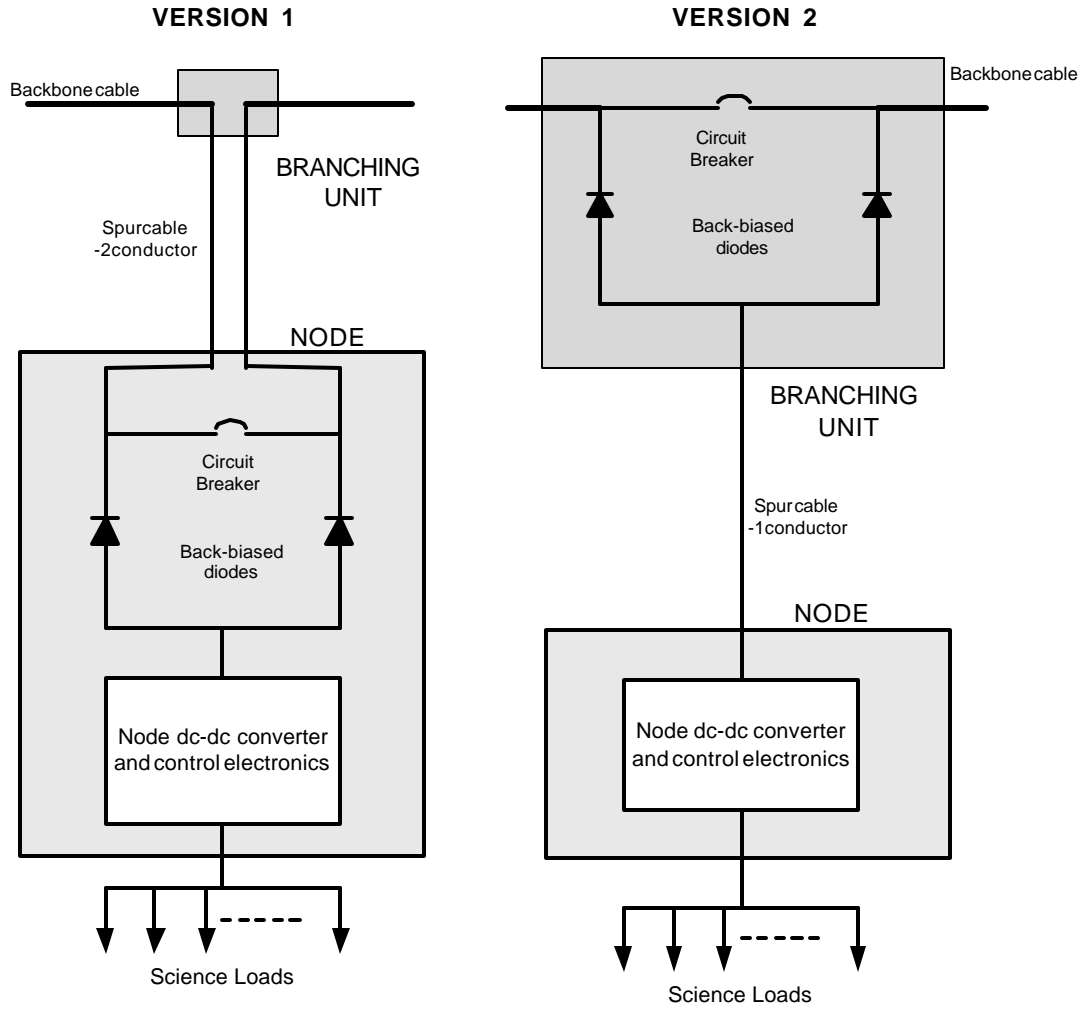


Figure 1.2 Version 1 and Version 2 power system designs

In both versions the power system is divided into two distinct parts – the power-delivering part and the load-serving part. The backbone cable and the branching unit (BU) are the power delivering part and the node with the associated load bus is the load-serving part.

In Version 1 a single node failure, particularly the failure of the dc-dc converter that feeds the load can cause failure to large sections of the network. A failed dc-dc converter will interrupt the node power supply. Thus the circuit breaker, which is normally open, cannot be powered. This will open the circuit breaker and isolate cable sections. In some circumstances, this could mean that large sections of the system are isolated. Another disadvantage of Version 1 is that it requires a costly two-conductor spur cable connecting the backbone to the node.

Version 2 is designed to be more reliable with a series power supply to drive the breaker and its electronics specifically. Any type of node failure, including failure of the dc-dc converter will affect that node only. It is also assumed that the circuit breaker, and its power supply and controls, can be built to be qualified for high reliability. Also, the spur cable connecting the branching unit and the node in Version 2 is a less costly single conductor.

Table 1-1 shows the comparison between the two design approaches. It indicates the advantages of one design over the other and the reason why Version 2 is the preferred choice for the NEPTUNE power system.

Table 1-1 Comparison of Version 1 and Version 2 power system designs

Version 1	Version 2
Conventional approach to power system design	Based upon the philosophy that cable faults are rare, but possible
Response to a fault is at the local level by the nearest circuit breaker	Response to a fault is at the system level by the shore station controls
Circuit breaker is complicated with many components	Complexity of circuit breaker is greatly reduced
Fault current is interrupted; arcing and restrikes are possible	Fault current is not interrupted; arcing and restrikes are not possible
Single node failure can cause failure in a large section of the network	Single node failure is not catastrophic for the system as that node only will be out of service
Reliability is low	Reliability is high

The dc switch or breaker constitutes a primary building block of the protection system in both Version 1 and Version 2 designs. The construction, functions and operating scenarios of the dc breaker of the NEPTUNE system are explored in depth in the following chapters.

Chapter 2. Version 1 Design of the NEPTUNE Power System

2.1 Introduction

The NEPTUNE power system, as currently envisioned, will cover a portion of the Pacific Ocean, along the western United States and Canada. It will extend from Victoria B.C. in the north to California in the south. The network will be laid out along the Juan de Fuca plate such that all the key geological and oceanographic features of this plate are within the reach of potential science users.

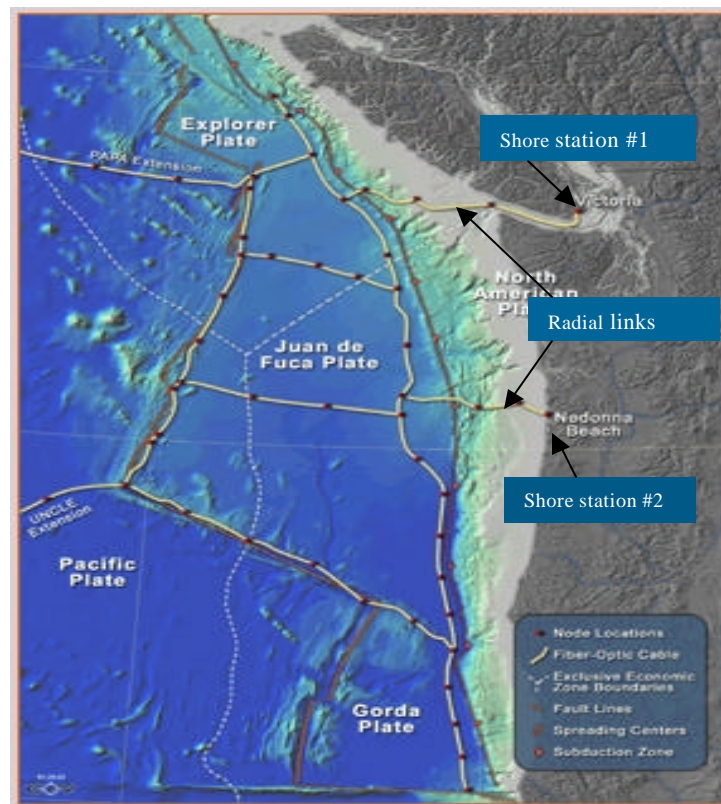


Figure 2.1 Structure of the NEPTUNE power system

The power system will use conventional telecommunication cable powered by two shore stations at 10kV each [4]. Under normal operating circumstances the cable will carry a steady-state current of 10A dc. The two shore stations will feed power into the main loop using two radial links (Figure 2.1). As each shore station power supply is 10kV, 10A rating, the entire power system will be consuming about 200kW of total power.

Loads will be connected in parallel; they may be purely resistive, variable resistance, motor loads or any combination of the above. The type and magnitude of the load is dependant on the user contract that will be finalized between the NEPTUNE administration and the ultimate science user. From a system point of view, the load can be assumed to be a power load consuming constant power.

To minimize the time and the extent of power outage following a cable fault, the backbone is sectionalized using circuit breakers. The circuit breaker, in the event of a fault, will isolate sections of the system before the overcurrent conditions cause any damage to system components. The circuit breaker is an important element of the power system from the protection point of view.

The NEPTUNE network will have circuit breakers placed roughly 100km apart. At these points of the network, the backbone will be branched out to serve the loads. The science loads are served at 400V dc. Multiple users can tap power from the backbone at the same junction point. Besides the dc-dc converter, the science node has control and protection circuitry. The supply bus for the science users will branch out of the node. The dc-dc converter provides the power supply for the node operations and also for the circuit breaker switches. Two redundant converters are placed in the node.

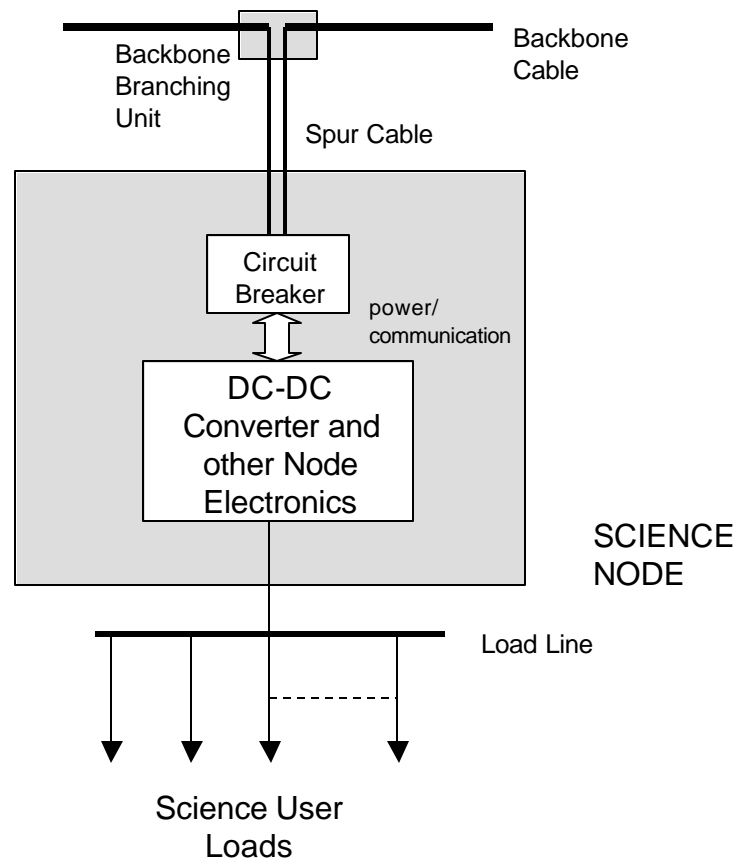


Figure 2.2 Block schematic for science node

In Version 1, the circuit breaker is also placed in the node unit (Figure 2.2). The backbone cable is split into a two-conductor spur cable at the backbone branching unit. The branching unit contains no active components. The node power system consists of the circuit breaker, the dc-dc converter and the control and protection circuits. These are located in the pressure cases of the science node and are fed via the spur cable. The science users are delivered power from the 400V load line.

2.2 Design of the DC Circuit Breaker

2.2.1 Basic Concepts

The science node consists of two diodes connected on both sides of a circuit breaker (Figure 2.3) [5]. The branching unit, converter and scientific instruments are all represented by the load box. After any of the adjacent nodes are energized, the given diode configuration allows the node converter to be powered from either side of the cable. Once the node converter is powered, the breaker logic circuit generates the closing sequence, thus making the power available to the next node.

Another function of the breaker is to disconnect sections of the cable system during faults or for system maintenance. The main problem with disconnecting dc current is the lack of zero crossing to extinguish the arc generated during the opening of the circuit breaker. Thus a bypass system needs to be implemented to achieve two objectives:

1. To force the current of the breaker to go to zero. This will make the breaker contacts separate without damaging arcs.
2. To prevent the breaker from restriking. This is a phenomenon that occurs after the breaker electrodes separate and the voltage builds up across its terminals exceeding the breaker's *withstanding voltage*. Restrikes reignite the arc inside the breaker and cause high frequency transients that could damage other components in the backbone system.

The switches used in the breaker circuit are vacuum switches, which are in normally open configuration. To close these switches, their solenoids are excited by dc current. The dc-dc converter in the node provides the power to operate these switches.

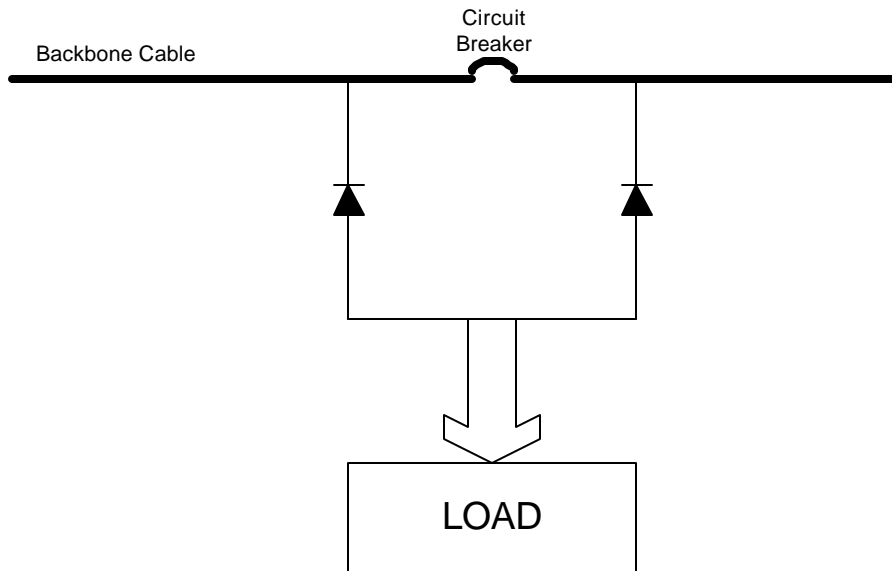


Figure 2.3 Conceptual schematic of the NEPTUNE node connected to backbone

2.2.2 Configuration of DC Circuit Breaker

In dc circuits, the current is continuous without zero crossings. Hence, unlike ac systems, interrupting the current cannot coincide with the natural zero crossing present in ac currents. In this case, the dc current must be driven to zero using external components before the interrupter is fully open.

One method to achieve this objective is to design a bypass circuit by which the current can be rerouted to a series capacitor. Because the capacitor interrupts the current when fully charged, the zero crossing can be achieved. The circuit breaker unit is composed of the following components:

- 1) 4 vacuum switches: S1, S2, S3, and S4 (Figure 2.4). The advantages of vacuum interrupters in medium voltage applications are widely recognized [6, 7]. They are normally smaller in size and lighter in weight compared with oil or air breakers. The vacuum switches are relatively fast (less than 20 msec) due to their small

moving parts and their short contact stroke. Furthermore, the contact erosion of the vacuum switches is minimal prolonging the lifetime of the switches. The sealed contact chamber of the vacuum interrupters contains all arcing, so they are relatively noise-free and safe to operate. Overall, vacuum breakers require less maintenance than most other types of breakers.

- 2) Soft-closing resistor R1
- 3) Bypass capacitor C
- 4) Discharging resistor Rd

The circuit breaker vacuum switches are normally open. On command, the vacuum switches are closed sequentially according on the needed operation. Three main operations of the breakers are:

- 1) Closing
- 2) Opening
- 3) Discharging

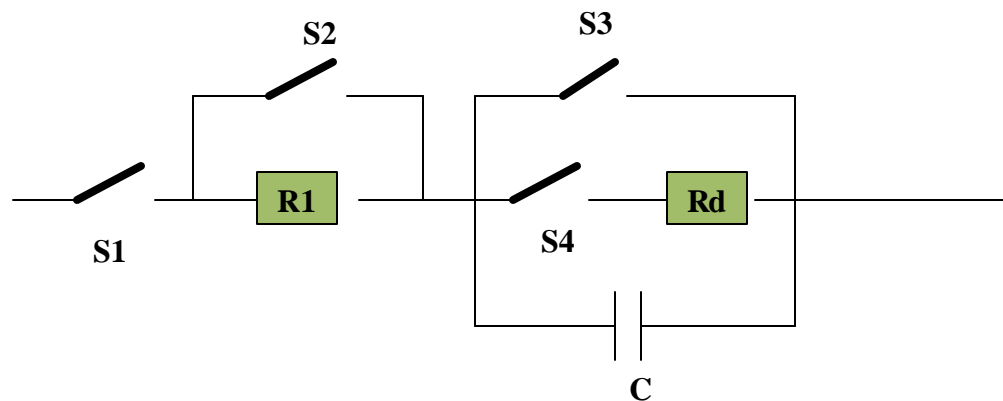


Figure 2.4 Components of dc circuit breaker

2.2.2.1 Closing operation

When the breaker receives a 'close' signal, it initiates the following closing sequence,

Step 1: Insert the resistance R1 to reduce the inrush current by keeping S2 open.

Step 2: Close S1 and S3 to energize the cable (Figure 2.5). The current flows through the soft closing resistor R1 to reduce the inrush current due to the cable capacitance.

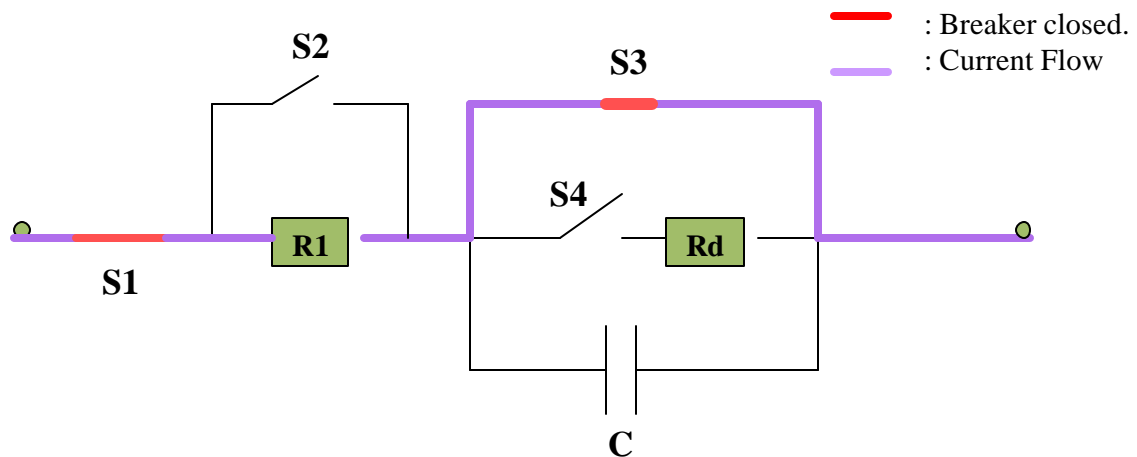


Figure 2.5 CB soft closing

Step 3: Remove R1 by closing S2 (Figure 2.6). The soft closing resistor (R1) is maintained in the circuit just long enough to reduce the inrush current. R1 is kept in the circuit for less than 1 s. More time is possible, but the resistance must have a higher energy rating.

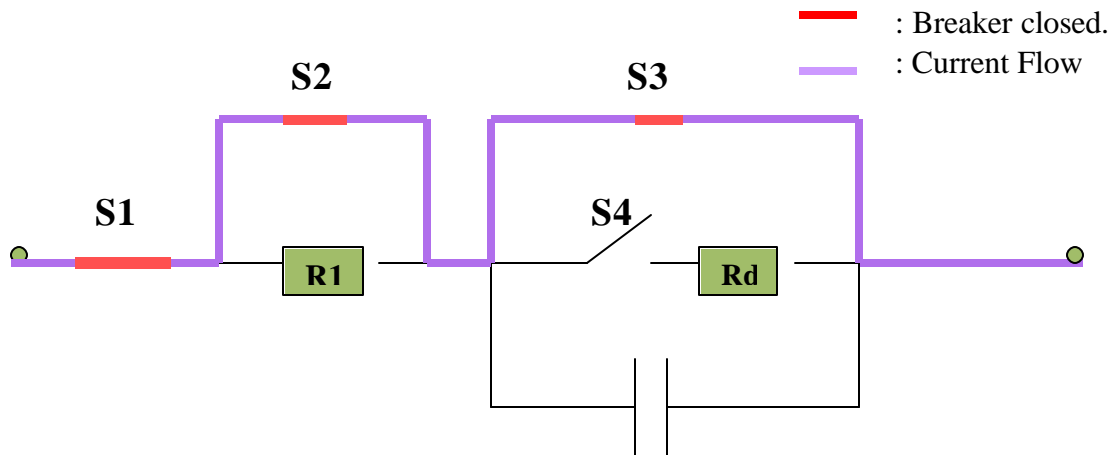


Figure 2.6 CB when fully closed

2.2.2.2 Opening operation

Upon receiving an opening command, the logic circuit of the breaker initiates a different sequence of switching.

Step 1: Open switch S3. In this process, the current will be routed through the capacitor (C) (Figure 2.7). During the charging process, the current of the cable is reduced exponentially. Once fully charged, the capacitor interrupts the cable current.

Step 2: Once the current is brought to zero, switch S1 can be opened and the circuit breaker is fully open.

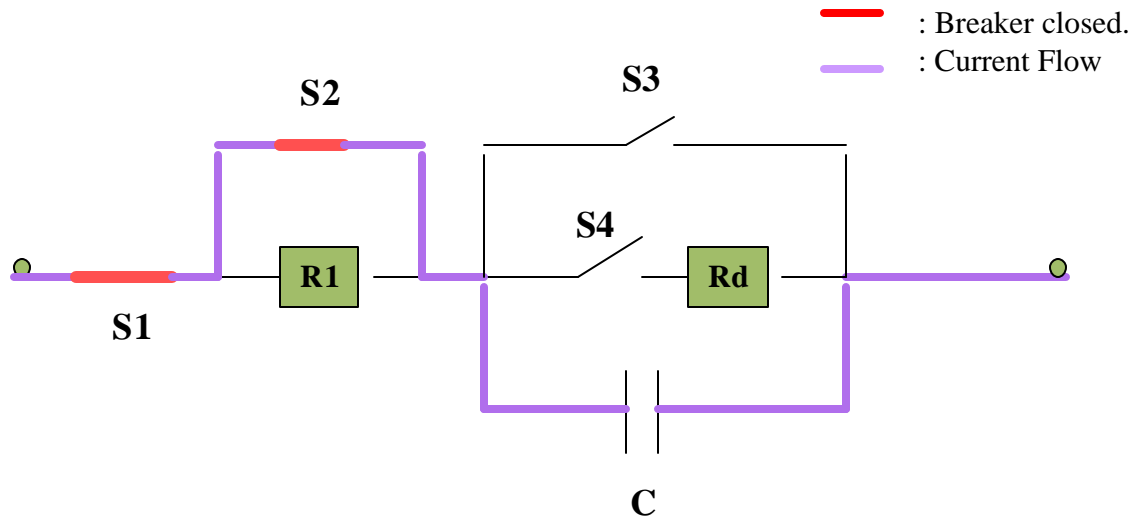


Figure 2.7 CB capacitor charging

2.2.2.3 Discharging operation

To reset the breaker for the next switching action, the capacitor must be discharged. This is done by closing S4, while the other switches are open (Figure 2.8). The capacitor is discharged through the resistor (R_d) whose magnitude determines the discharging time of the capacitor.

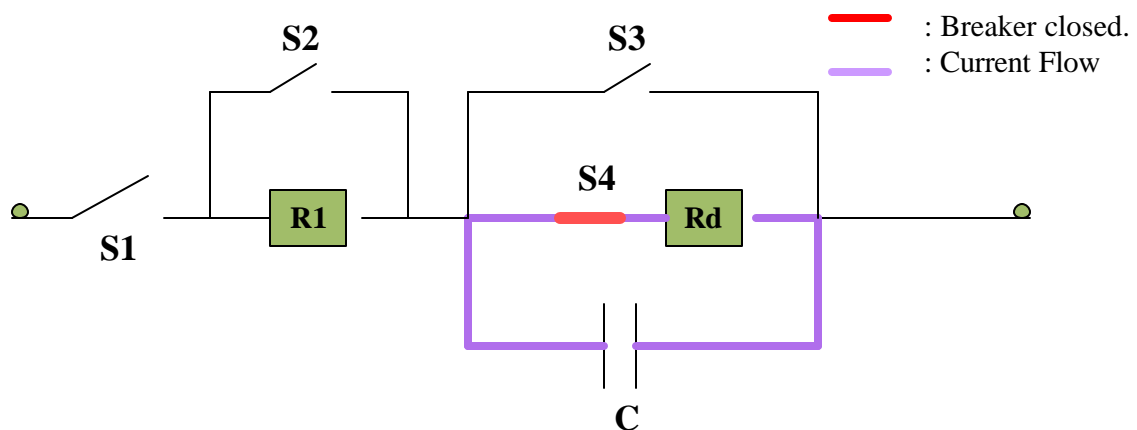


Figure 2.8 CB capacitor discharging

2.3 Hardware Development of the DC Circuit Breaker Prototype

It is necessary to validate the Version 1 design with a hardware prototype thus demonstrating that the design is physically viable and will work under the specified operating conditions. The prototype is a low voltage stand-alone circuit breaker connected to a 300V dc source. The testing is carried out for varying loads. The standard test voltage is 125V and the standard test current is about 5A.

2.3.1 300V lab prototype

The circuit breaker (Figure 2.4) is built in the laboratory for analyzing its functions and operations.

The circuit breaker components are:

- Vacuum switch (4)

Manufacturer: Jennings Tech. RF71-12S

Maximum rated voltage: 12kV

Rated Current: 15A

Type: Single pole single throw (SPST) and Normally open (NO)

Release time: 3ms

- Capacitor (1)

Value: 1 μ F

Maximum rated voltage: 500V

- Resistors (2)

Soft-closing resistor.

Value: $1\text{k}\Omega$ at 500V

Load resistance

Variable Value: 20Ω - 1000Ω at 500V

- Power Source

Value: 300V DC at 50A

The test conditions were as follows:

Test voltage: 125V

Test Current: 5A

The breaker circuit is tested by running through all the stages of the breaker's operation as indicated in Figure 2.5 through Figure 2.8.

The durability of the vacuum switches is tested by cycling through the different circuit breaker stages continuously.

2.3.2 Vacuum switch drive circuit

The vacuum switches in the circuit breaker are normally open (NO) switches. The status of the vacuum switches is controlled by solenoids. The solenoid for each vacuum switch is incorporated within the switch unit.

The solenoid is a coil with a large reactive component. For a NO switch, when the solenoid is *not* excited, the switch remains open; when excited, the switch closes.

For the vacuum switch under test, the solenoid has a driving voltage of 12V. Its equivalent impedance is 48Ω . The solenoid of each vacuum switch is excited by 12V, 250mA. With four vacuum switches in the breaker design, the drive circuit will require an auxiliary power supply of 12V, 1A.

The drivers for the vacuum switches solenoids are MOSFETs, as they are highly reliable for switching actions, with minimal losses. The MOSFET chosen for the lab prototype is the *IRF840*, manufactured by International Rectifiers. It is ideal for high switching applications and has very small on-state resistance. The nominal gate-source voltage for the MOSFET is about 12V.

A control logic (TTL / EPROM) drives the MOSFETs, which in turn controls the respective vacuum switches. The control logic is based upon the different breaker stages (See Section 2.2). The test setup can be differentiated into three distinct parts:

- *Power Circuit*, including the vacuum switch, 300V dc supply and the 5A load
- *Drive Circuit*, including the MOSFETs driving the solenoids and the auxiliary power supply
- *Logic Circuit*, the low power control circuitry

The low power control logic circuitry is highly sensitive to electromagnetic interference (EMI). The power supplies of the power circuit and the drive circuit can be very noisy. Also, the loads in the drive circuit are highly inductive and, due to the continuous switching, produce very large current spikes. All these factors necessitate the isolation of the low power logic circuit with *opto-isolators* (Figure 2.9) from the rest of the test setup.

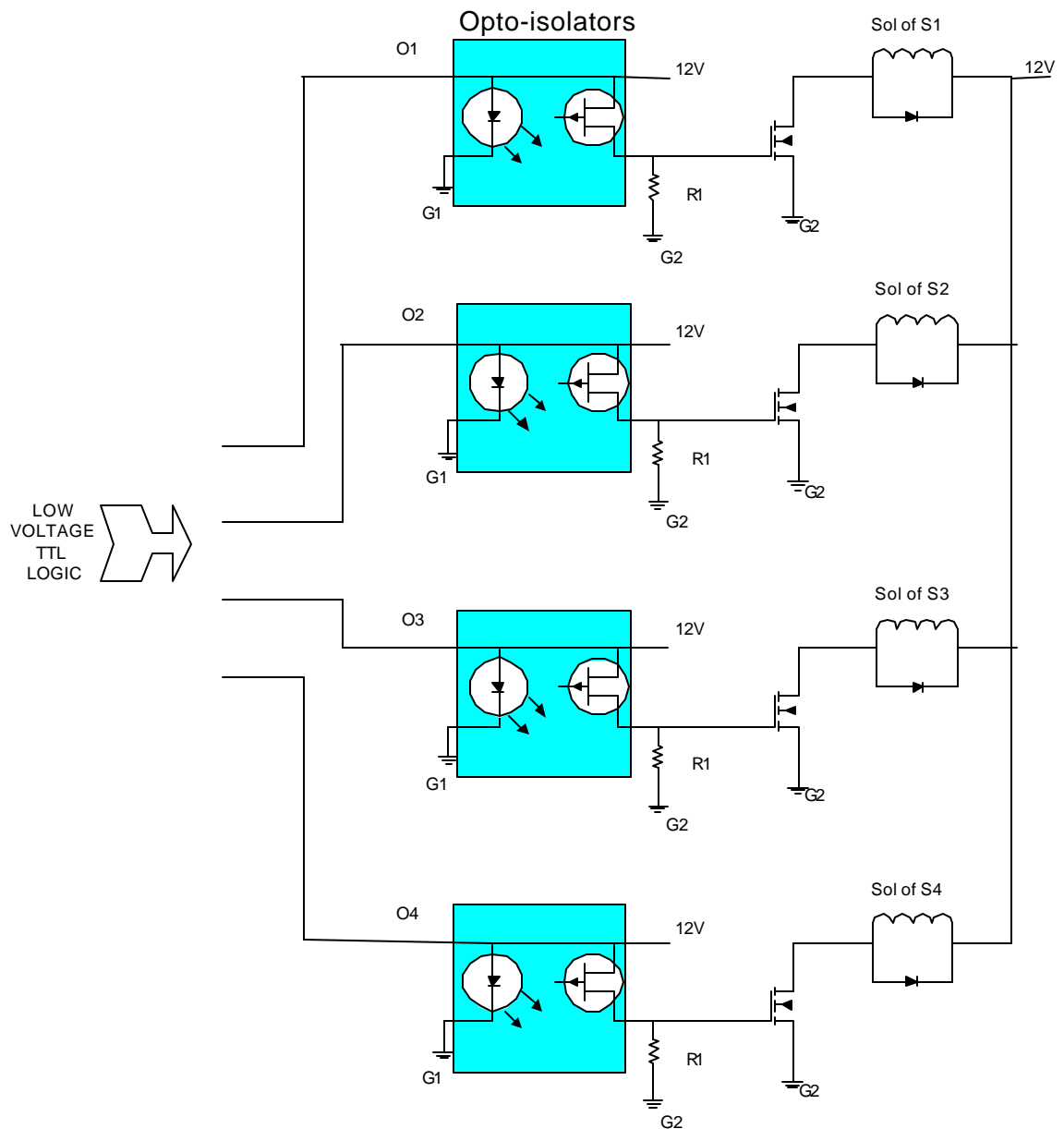


Figure 2.9 Circuit diagram for driver circuit

2.3.3 Logic circuit

In the test setup, the aim is to test the vacuum switches for their reliability and durability. Thus the circuit breaker is switched through its different stages continuously in a cyclic

fashion. The discharging operation of the previous cycle is followed by the closing operation of the next cycle. Table 2-1 explains the status of the four different switches in each stage of the breaker operation, where a closed switch is represented by '1' and an open switch by '0'.

Table 2-1 Logic for switch operation in circuit breaker

Stage	Description		S1	S2	S3	S4
1	Closing Operation	Soft closing	1	0	1	0
		Closed Circuit	1	1	1	0
2	Opening Operation		1	1	0	0
3	Discharging Operation		0	0	0	1
4	Open Circuit		0	0	0	0

The logic circuit is devised such that it follows the truth table (Table 2-1) and loops around continuously until a command is given to stop the test. Two options were considered for the design of the logic circuit.

Option 1: TTL Logic

This option utilizes the TTL devices such as OR gates, AND gates and binary counters to construct the desired logic circuit (Figure 2.10). The circuit operates on a clock signal, which is generated by the frequency generator or an IC 555 timer circuit. The circuit

starts operating on the activation of the clock signal and stops operating when it is deactivated.

The clock signal is fed to the binary 8-bit counter. It counts through the different breaker stages and in the process generates three input signals for the AND-OR logic. The logic generates four output signals, one each for the control of the respective MOSFETs in the driver circuit. The output of the logic circuit is isolated from the input of the driver circuit by opto-isolators.

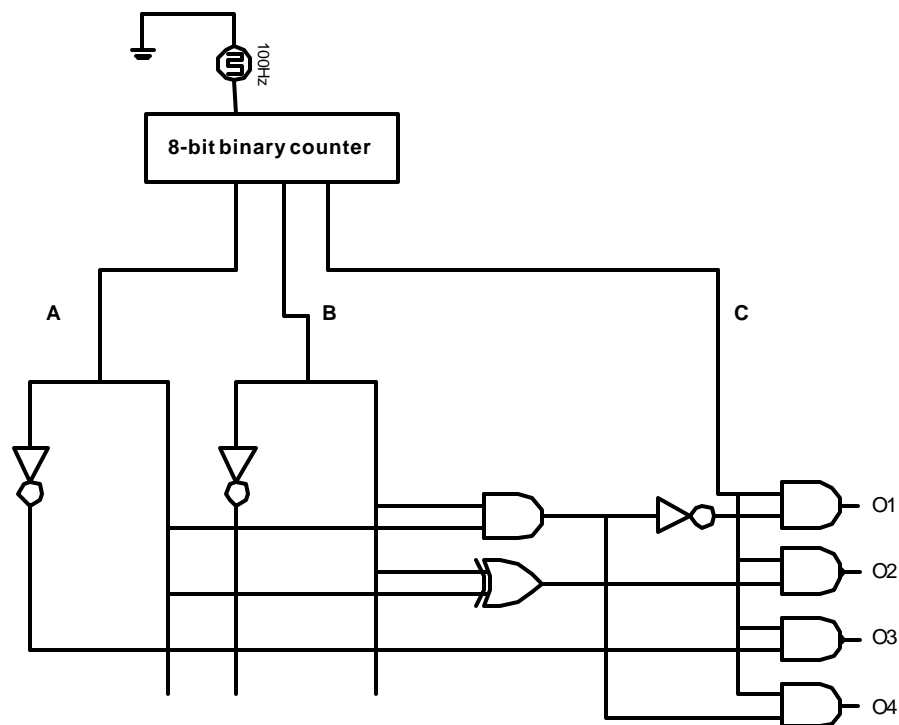


Figure 2.10 Circuit diagram for TTL control logic

Option 2: EPROM Programming

EPROM chips can be programmed as a state machine that continuously loops around the states of the circuit breaker (Table 2-1). The chips are Generic Array Logic *GAL2210*

ICs, manufactured by Lattice Semiconductors. They are programmed using Verilog HDL, which is a hardware description language used to design and document electronic systems. The input to the chip is the clock signal generated by a frequency generator. The outputs of the chip are the four signals that control the respective MOSFETs in the driver circuit.

2.3.4 Results of lab testing

Continuous Voltage: 125 V

Continuous Current: 4.5 A

Total Breaker Cycles: 125,000

Normal cycle switching frequency: 20 Hz

Maximum cycle switching frequency: 100 Hz

Maximum tested voltage: 200 V

Maximum tested current: 5 A

Chapter 3. Version 2 Design of the NEPTUNE Power System

The concept of Version 2 design on the NEPTUNE power system is introduced in Chapter 1. The description of the various circuits and algorithms implemented in Version 2 design are explained here.

3.1 Branching Unit Circuit Description

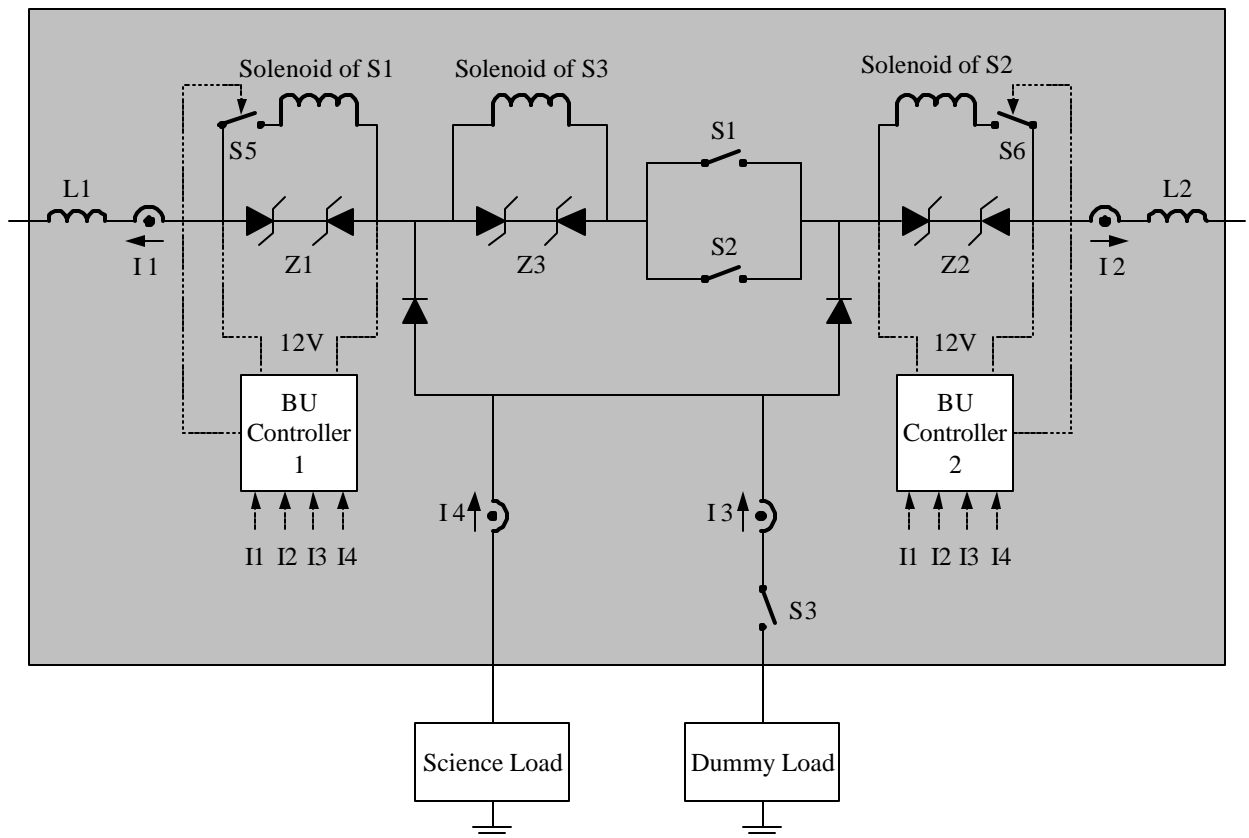


Figure 3.1 Branching unit circuit diagram

The Version 2 branching unit (Figure 3.1) is powered by zener diodes in the backbone circuit. Z1, Z2 and Z3 are the three pairs of back-to-back zener diodes acting as series

power supplies. Z1 and Z2 power the two BU controllers, which are responsible for the control actions. The functions of the BU controller and the algorithms that govern them are described in Section 3.3. Z1, Z2 and Z3 also power the solenoids of the three vacuum switches S1, S2 and S3. S1 and S2 are the backbone switches and are connected in parallel so that the closure of any one will close the BU. This arrangement is necessary as the initial powering of the BU can be from either side.

The dummy load is present and active only during special modes of the system operation. Also, they are activated when the science load is not drawing enough current to keep the BU series power supply active. The current sensors I1, I2, I3 and I4 measure the current in every branch of the BU and the BU controller initiates their control actions based upon these current measurements. There are no voltage or power measurements within the BU and there is no communication within or outside the BU. The BU controller is thus essentially isolated. L1 and L2 are surge compression coils sized 100 μ H each.

3.1.1 Series power supply

In the Version 2 design of the NEPTUNE power system, the branching unit is co-located with the node and the science loads. This is similar to Version 1, but the switches in the BU are powered by a local power supply.

The power supply is comprised of a series-connected, reverse-biased zener diode. This zener diode is placed in the backbone and maintains a constant voltage of around 12V across it in the reverse region of its characteristic curve. The system current flows through the zener diodes. This current is typically around 2-5A for a BU not in the radial links of the network. As such, the zener diodes can function as series power supplies of about 24-60W, depending upon the BU location.

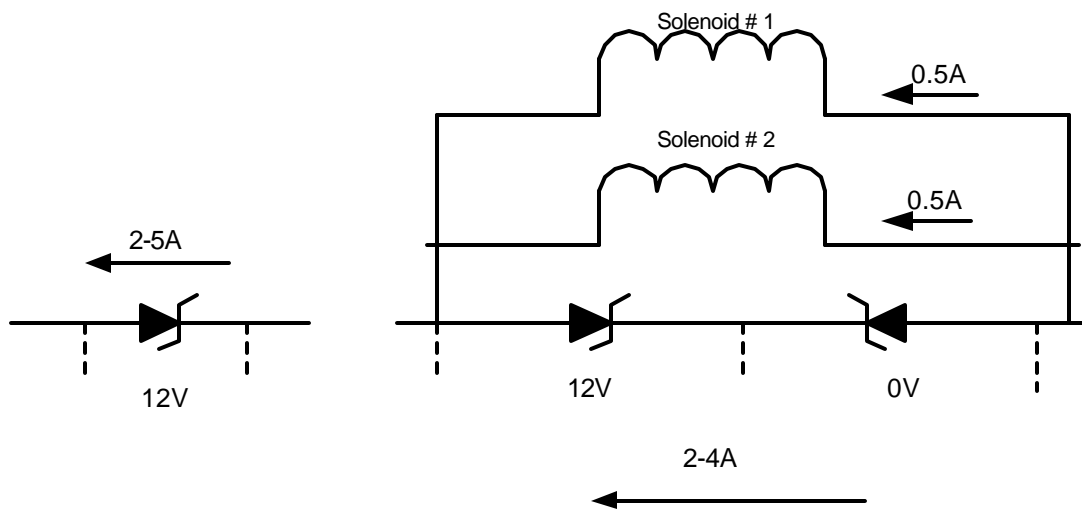


Figure 3.2 Zener series power supply

The solenoids of the vacuum switches are connected across the reverse biased zener diode. These solenoids will typically draw 0.5A current.

In the NEPTUNE power system, the direction of current flow can be bi-directional, depending upon the status of the various science loads and the system configuration. The series power supply powers the switches irrespective of the direction of current flow. This is done by having two back-to-back zener diodes (Figure 3.2). Irrespective of the direction of current flow, either of the two zener diodes will operate in the reverse region of its characteristic curve. This zener diode will power the switches in the BU.

3.2 Modes of System Operation

The Version 2 NEPTUNE power system has four distinct modes of operation:

1. Normal
2. Fault
3. Fault-locating

4. Restoration

Each of these modes of operation is explained in the following.

3.2.1 Normal mode

In the normal mode, the NEPTUNE power system is managed by PMACS (Power Management and Control System). The data for the calculations is obtained from the science node, as there is no communication with the BU. PMACS also utilizes state estimation to develop a model representing the system status at the shore station.

The objective in the normal mode of operation is to provide power to the science loads at each of the nodes in the NEPTUNE network. In this mode, the system is under normal condition with no faults. The zener valves in the backbone circuit are located in the BU. The voltages across the zeners drive the solenoids of the vacuum switches.

3.2.2 Fault mode

The objective of this mode of operation is to trigger a system shutdown in the event of a fault, and to protect system components by limiting the fault current. Cable faults along the backbone are assumed to be rare, but possible. In the event of a backbone cable fault, a large fault current may flow through some of the electronics in the BU. The magnitude of the transients depends upon the cable parameters. The charged energy in the cable capacitance will be discharged into the fault, resulting in large di/dt and dv/dt values.

If a fault occurs, the shore station disconnects the entire system. The BU controller remains passive during faults and the backbone switches remain closed. The shore station determines the presence of a fault by at least one of the following methods:

1. The fault current is sensed at the shore station if the fault is near the shore station
2. The nodes around the fault experience a drop in voltage and send this information to the shore station

3. If the node voltage drops to a very low value and the nodes cannot communicate with shore anymore, PMACS determines the presence of the fault based on system analysis

When the fault occurs, the shore station switches off the power supply causing the entire NEPTUNE system to shut down.

3.2.3 Fault locating mode

The objective of this mode is to locate the fault with no communication between the BUs or between the BUs and the shore. After the system is shut down due to the presence of a fault, the shore station supply is tripped, and the backbone switches in all the BUs are open, with the exception of the dummy load switches, which are normally closed.

The shore station energizes the system at a voltage lower than the pickup voltage of the node dc-dc converters (5.6 kV) to isolate all science loads. Because the BU has no communication with the shore station or any other node, the magnitude of the voltage across the dummy load is used by the BU controller to determine the intended mode of operation. For example, for fault-locating mode, the shore station voltage can be set at about 2.5-3.5 kV, and for restoration mode, the shore station voltage can be set at about 5 kV.

3.2.4 Restoration mode

The objective of this mode is to energize the system and isolate any faulted section without PMACS or shore station intervention. If a fault exists, the location of the fault is unknown to the BU controller.

In the restoration mode, the system is energized at about 5 kV to isolate the science node, and to tell the BU controller that the intention is to restore the system and isolate any faulted section of the cable.

Before the system enters the restoration mode, the system has been completely powered down after the fault-locating mode. The shore station voltage is initialized to about 5kV. The BUs are energized in a sequential manner. Whenever a BU is energized, the BU controller takes appropriate control actions depending upon the circuit conditions. At the end of the restoration mode, all the system BUs are energized and the faulted cable section has been isolated. After the restoration mode, the shore station voltages are raised to 10kV and the system re-enters normal mode.

The overall system control algorithm is summarized in Figure 3.3. The power system is in the normal mode most of the time. Once a fault occurs, the PMACS detects it and causes system shutdown. The system is re-energized in the fault-locating mode at low voltage (about 2.5-3.5 kV). In this mode the state estimation at the shore stations locates the fault. The system is then shut down and is re-energized in the restoration mode at about 5kV, where the system is completely energized and the fault is isolated. The shore stations then raise their voltages to the nominal 10 kV. After the faulted cable is repaired, the system is shut down and re-energized again in the fault-locating mode.

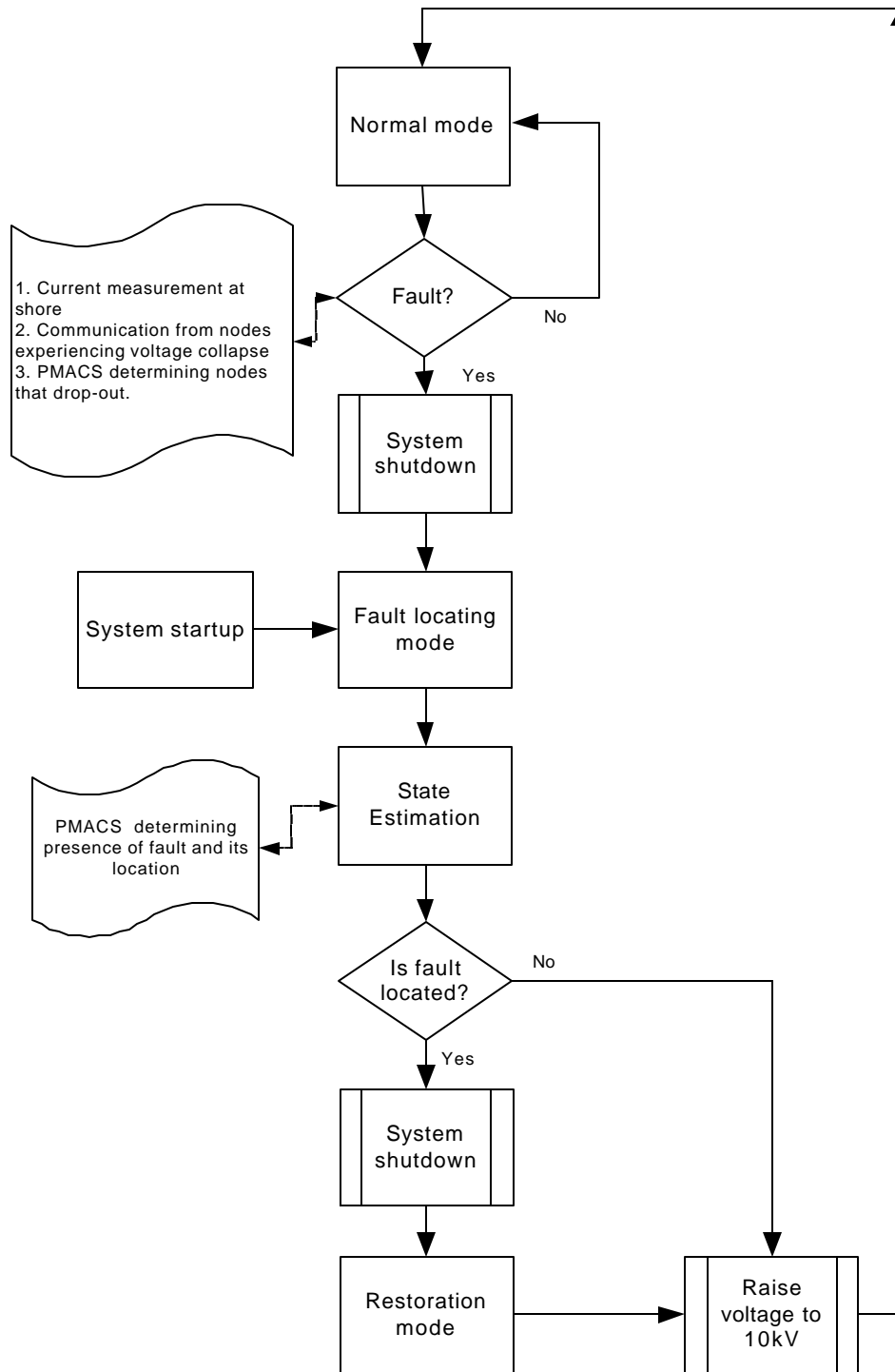


Figure 3.3 Overall system control actions

3.3 Algorithms for Branching Unit Controller

The normal mode and the fault mode are passive modes for the BU controller. The BU controller does not initiate any control action in these two modes. In the normal mode, all the BU controllers of all the BUs keep the S1 and S2 backbone switches closed and the S3 dummy load switch open. In the fault mode the BU controllers of some BUs may sense overcurrent. But they do not respond to this overcurrent and are passive during fault mode. The response to a fault is a system level control action. PMACS detects the fault using its system analysis software and shuts down the shore station power supplies. This causes the entire network to de-energize and the series power supplies of all BUs to shut down and deactivate the BU controllers.

On re-energization the default mode of operation for the BU controller is the fault-locating mode.

3.3.1 Fault-locating mode

Before entering this mode of operation, the system is completely shutdown. The backbone switches are open and the dummy load is connected to the circuit. The shore station voltage is initialized at 2.5-3.5kV.

Figure 3.4 shows a section of the system and the control function of the BUs under fault conditions. The main steps of the fault-locating mode are shown in Figure 3.5. The switches of all dummy loads are closed (default position).

When the first BU is energized, its dummy load causes current to flow in the zeners. The BU controller waits for the transients to subside (Delay1), then measures the current into the dummy load. Because the dummy load resistance is known apriori, the voltage at the BU can be computed by the controller, and the controller determines that the mode of

operation is the “fault-locating mode.” The BU controller closes its backbone switch (S1 or S2).

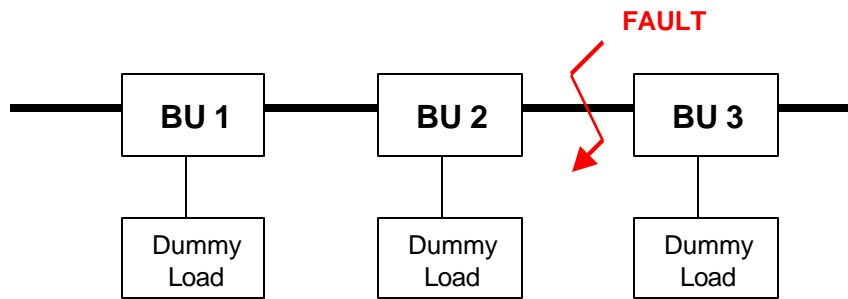


Figure 3.4 Typical setup in fault-locating mode

After another delay (Delay2), equivalent to the closure of at least two more BUs, the dummy load of the current BU is disconnected.

The closing process continues until all BUs are closed including the ones adjacent to the faulted section of the cable. The BU controllers will keep closed the backbone switches even in the presence of a fault. This is done to allow PMACS to identify and locate the fault.

3.3.2 Restoration mode

In the restoration mode, the system is energized at about 5 kV to isolate the science node, and to tell the controller that the intention is to restore the system and isolate any faulted section of the cable. The steps of the restoration mode are shown in Figure 3.6.

- The dummy load (Figure 3.1) is always in the circuit because S3 is normally closed.

- When the zeners of the first BU are in their constant voltage region, the BU closes its backbone switch after a delay (Delay1) to allow for the transients in the upstream section to die out.
- If the BU closes on a healthy cable section, the current of that section is the cable charging current plus the dummy load current of the next BU. The transient in current should subside after a certain time. The controller senses this current and evaluates its magnitude after it reaches the steady state.
- If a BU closes on a faulted section, the current sensed by the BU will be higher than that for the unfaulted cable. If the current sensed by the BU remains high after the delay (Delay1), the BU controller considers the switched section of the cable faulted. The BU controller will then open its backbone switches S1 and S2, and will not allow them to close unless the system is shut down and the controller is reset to either “fault-locating mode” or “restoration mode”.

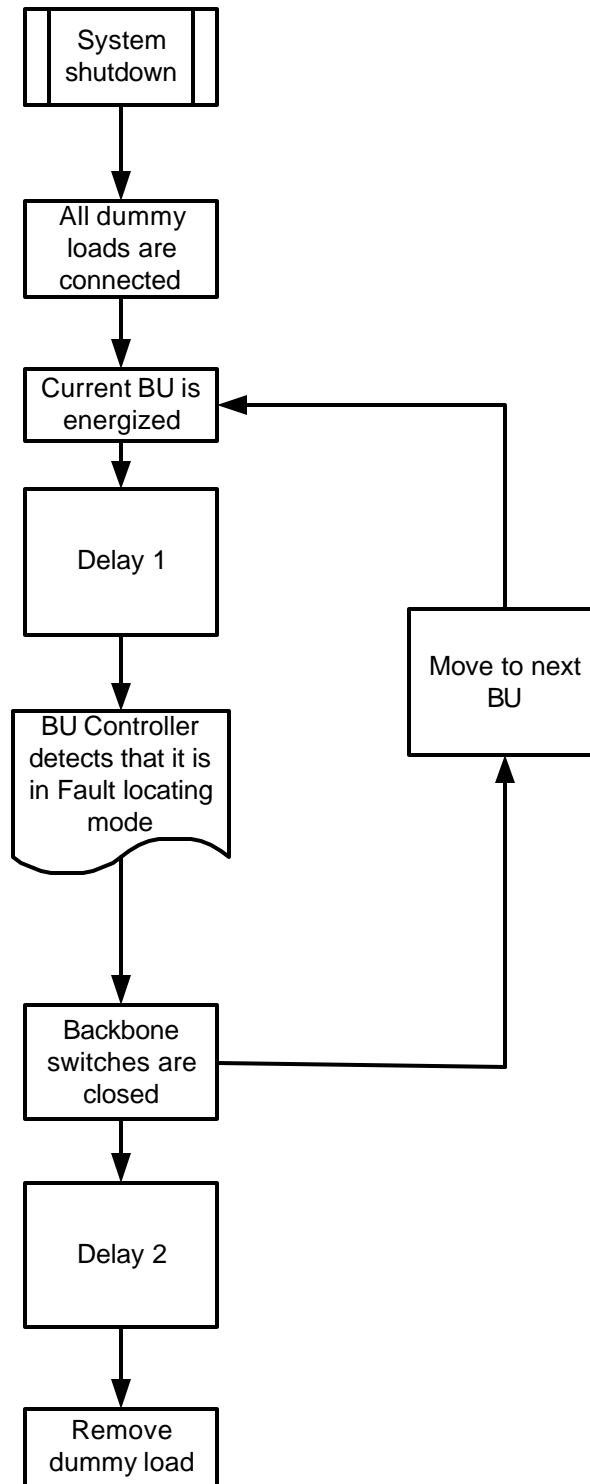


Figure 3.5 Steps in fault-locating mode

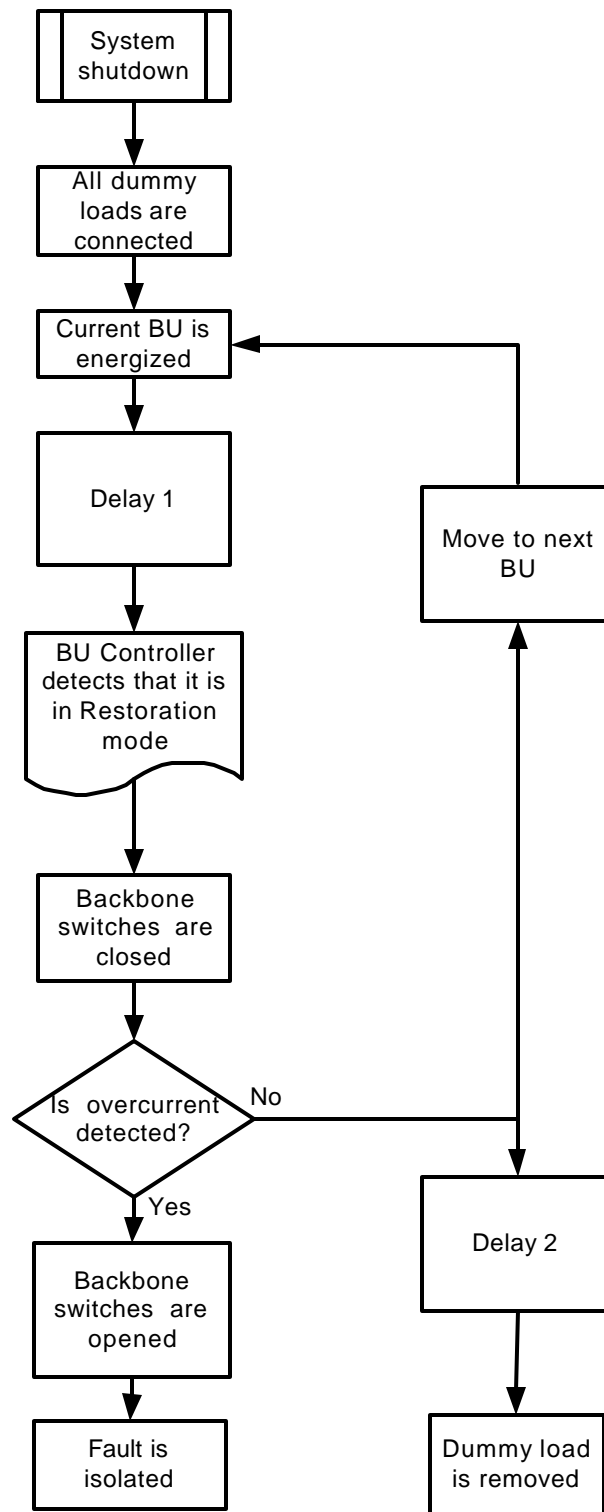


Figure 3.6 Steps in restoration mode

Chapter 4. Electromagnetic Transients Analyses

4.1 Introduction

The most commonly occurring transients in a power system are switching transients. These transients occur when the system topology is changed due to some switching action. A large power system contains many circuit breakers and these are regularly switched to isolate sections of the power system for maintenance or other purposes. When these circuit breakers are switched, the system topology is changed, and in the process of moving from one steady state to another, electromagnetic transients are produced.

The most basic representation of a high voltage circuit breaker closing into a short-circuited transmission line is a sinusoidal voltage source, switched onto a series connection of an inductance and a resistance (Figure 4.1).

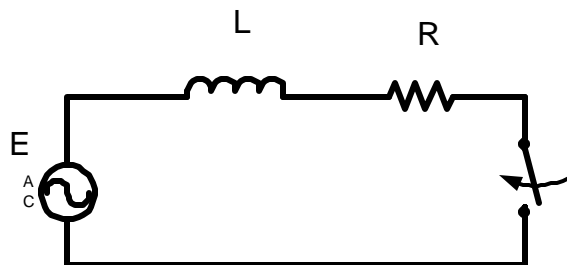


Figure 4.1 Switching in RL series circuit

The voltage source E represents the generator, L represents all the inductive elements in the power system, including the synchronous reactance of the generators and the inductance of the transmission line, and R represents the resistive losses of the system.

The non-homogenous differential equation for the circuit is:

$$E_{\max} \sin(\omega t + \mathbf{f}) = Ri + L \frac{di}{dt} \quad (4.1)$$

The switch can close the circuit at any instant and the phase angle can have a value between 0 and 360°.

The description of the solution to the differential equation (4.1) is given in [8]. The current in the circuit contains a decaying dc component and an ac component. The initial value of the dc component depends upon the instant of circuit closing.

The current in the circuit after closing the switch is asymmetrical. In case of no transient oscillations, the current immediately reaches steady state and becomes symmetrical. The asymmetrical current in the circuit can reach a peak value of nearly twice that of the symmetrical current, depending upon the value of the time constant L/R.

Applying this analogy to a high voltage power system like NEPTUNE, we see that when a circuit breaker closes on a long, unenergized cable, strong stresses will act on the components and cables due to the large inrush currents. These stresses may lead to insulation breakdown due to overvoltage, or may cause overheating of components due to overcurrents. High di/dt and high dv/dt are also damaging to the system components. Thus it is extremely crucial for the design of any power system to analyze the various transient conditions that may be experienced. The various components of the power system must be designed to withstand these transient conditions.

4.2 Dynamics of the NEPTUNE Power System

There are 48 nodes in the entire NEPTUNE power system, collocated with circuit breakers (Figure 4.2). A fault at any place in the network will initiate some control action. This could include the opening of the nearest circuit breakers in Version 1. In Version 2, at the shore station PMACS detects the fault and shuts down the system.

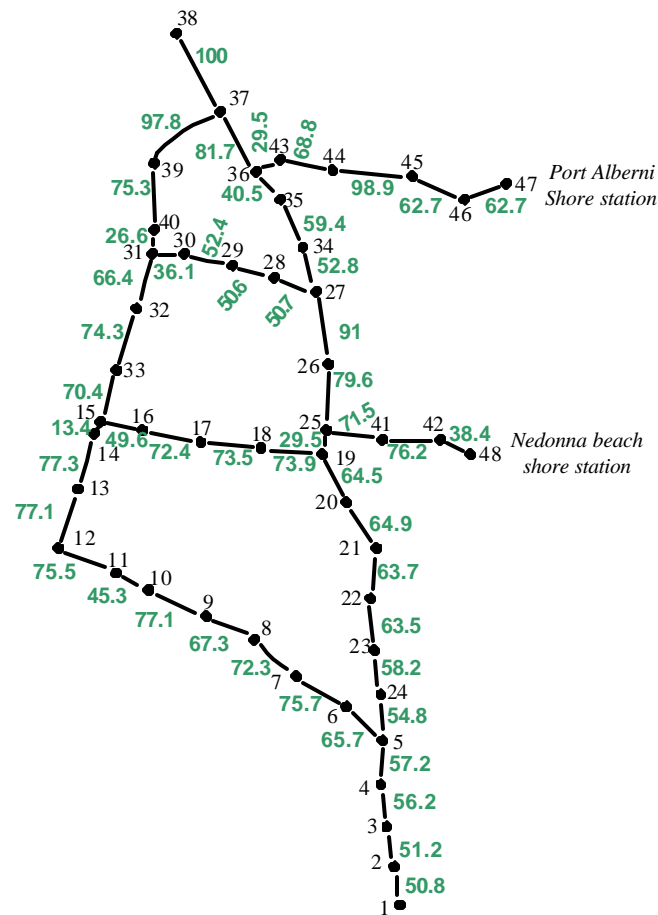


Figure 4.2 Node locations and relative distances in km

A bolted phase to ground fault is the worst-case scenario. The occurrence of the fault causes overcurrents and overvoltages. In Version 1, when the circuit breaker at any node location opens to isolate a fault, it is interrupting a large magnitude of current. In a dc system the fault current does not have a naturally occurring zero. This causes arcing and restrikes at the circuit breaker.

In Version 2 the problem of arcing and restrikes is solved. The circuit breakers operate only after the system is de-energized. However, the circuit breaker at the shore station interrupts fault current and experiences the same arcing and restrikes.

The worst-case scenario for a cable fault is a fault close to the shore stations. Here, the equivalent impedance from the shore to the fault location is very small. Thus the transient

currents will have a very high magnitude. Moreover the charged cable capacitance of the entire network will try to discharge its stored energy into the fault.

If the location of the fault is further away from the shore, the equivalent cable impedance in the circuit increases. This reduces the magnitude of the fault current, because the equivalent circuit has a larger cable inductance. The modeling of the power system and its transient analysis for various worst-case scenarios is done using Electromagnetic Transients Program. The simulation results are included in Chapters 6 and 7.

4.3 Electromagnetic Transients Program (EMTP)

The recent availability of greater computational power has greatly advanced the development of numerical simulation techniques. The computer program most widely used for the simulation of electromagnetic transients is the *Electromagnetic Transient Program* (EMTP). EMTP was created by H.W. Dommel for the Bonneville Power Administration (BPA) [9]. EMTP is available as the freeware Alternative Transients Program (ATP). The commercial version of EMTP (EPRI/EMTP) is developed by the Electric Power Research Institute (EPRI). Another popular version of EMTP is EMTDC (Electromagnetic Transients for DC Systems), developed by Manitoba High Voltage dc (HVDC). The present work has used ATP-EMTP for simulation purposes.

The EMTP uses the trapezoidal rule of integration (4.2) to convert the differential equations of the network components to algebraic equations.

$$\frac{x(k) - x(k-1)}{t} = I \frac{y(k) + y(k-1)}{2} \quad (4.2)$$

Nodal analysis techniques are used by EMTP for the simulation of electromagnetic transients. This makes the construction of the mathematical model straightforward and based upon simple rules [10, 11].

An electrical network consists of branches that are interconnected by nodes. The network can be described by

$$Y_B v_B = j_B + i_B \quad (4.3)$$

where v_B is the vector of nodal voltages of the branch, j_B is the vector of source dependant (history) nodal current injections, i_B is the vector of currents flowing into each branch and Y_B is the nodal admittance matrix of the branch [4].

In equation (4.3) shows that the complete network is represented in terms of the branch admittances and the history current sources represented by vector j_B . Knowing the current injections into a particular branch can help in finding the nodal voltages and vice versa.

The basic structure of the actual computation works as follows:

- The Y-matrix is constructed based upon the network topology and then inverted using memory efficient methods
- The time loop is entered and the vector of current injections and vector of history current sources is calculated
- The set of linear equations described in (4.3) is solved using the inverted Y-matrix, to find the vector of nodal voltages
- The history current source vector j_B is calculated for the next iteration in the time loop
- Once the time loop is completed the results are displayed in appropriate format

Thus, linear elements such as resistances are represented by their corresponding admittance values. The non-linearity introduced by elements such as inductors and capacitors is represented by their *associated discrete circuit models* (ADCM) [11]. The ADCM of each non-linear element is dependant on the particular integration method used.

For the modeling of diodes and other switching elements piecewise linear approximation is normally used. Modern day simulators have advanced interpolation and compensation methods to prevent numerical instability.

The description of the development of the numerical models for any component used in power systems is given in [12]. It describes the modeling of resistances, capacitances, inductances, transformers, transmission lines, cables, switches, motors and control systems.

4.3.1 Cable models in EMTP

In all electromagnetic transient simulators, there are two principal methods to represent transmission lines. For steady-state analysis PI line sections are used. This lumped parameter approach is also used in transient simulations, especially when the lines are short in length. The second method is to use distributed parameters, which are most suited for transient response. These models operate on the principle of traveling waves. A voltage disturbance will travel along a conductor at its propagation velocity until it is reflected by the other end of the line. Most advanced distributed parameter models use methods to prevent numerical instability while maintaining the accuracy of results.

The ATP-EMTP has various models to represent cables. These models can account for arbitrarily shaped cables, snaking of cables, etc. The user can select any of the several models for cables such as lumped or distributed parameters; frequency independent or frequency dependent models [12, 13]. The choice of cable model is dependent on a number of factors such as the length of the cable, the nature of the simulation (fault, surges, etc) and the fidelity of the results. The following are the various options for cable models:

- 1) *Bergeron*: Distributed parameter model including the traveling wave phenomena. However, it represents the line resistances as lumped elements.

- 2) *PI*: Nominal PI-equivalent model with lumped parameters, which is suitable for short lines.
- 3) *Noda*: Frequency-dependent model. This algorithm models the frequency-dependent transmission lines and cables in the phase domain.
- 4) *Semlyen*: Frequency-dependent simple fitted model. The Semlyen model was one of the first frequency-dependent line models. It may give inaccurate or unstable solutions at high frequencies.
- 5) *JMarti*: Frequency-dependent model with constant transformation matrix that is suitable for simulating traveling wave phenomena in long cables.

4.3.1.1 *Brief description of the JMARTI model*

In 1982 J.R. Marti developed his model for accurate representation of transmission lines. Most of the previous line models were frequency-independent and hence could not simulate the response of the line over a wide range of frequencies. The accuracy of the results in most transient studies was poor. Efforts to develop frequency-dependant line models resulted into models, which were numerically unstable.

J.R. Marti's new model was numerically stable and was generic enough to be applied for many different cases [14]. In the JMarti model, multiphase lines are first decoupled through modal transformation matrices so each can be studied as a single-phase circuit. Here, an innovative method of fitting the numerical results adapted the simple concept of asymptotic fitting introduced by Bode [15].

The JMarti model [14] is selected for the NEPTUNE simulations because it is fast and the most reliable algorithm developed for accurate modeling of transmission lines over a wide frequency range. The routine is numerically robust compared to earlier algorithms.

The disadvantage of this method is that it uses a constant frequency independent transformation line and could be inaccurate for unbalanced, untransposed lines and underground cables. In case of the NEPTUNE cable, the analysis has to be single-phase and so the transformation matrix does not affect the accuracy of the simulation.

4.3.2 TACS and MODELS

The Transient Analysis of Control Systems (TACS) Module in ATP is suitable for simulating several complex systems such as HVDC converter controls, excitation systems of synchronous machines, power electronics and drives, electric arcs (circuit breaker and fault arcs) and devices or phenomena that cannot be modeled directly with existing network components.

The control system devices and phenomena modeled in TACS and the electric network are solved separately. Output quantities from the network solution can be used as input quantities to TACS at the same time step. But, the output quantities from TACS can become input quantities to the network solution only over the next time step (Figure 4.3). The electrical network and TACS can exchange signals such as node voltage, switch current, switch status, time-varying resistance, voltage, and current sources [12].

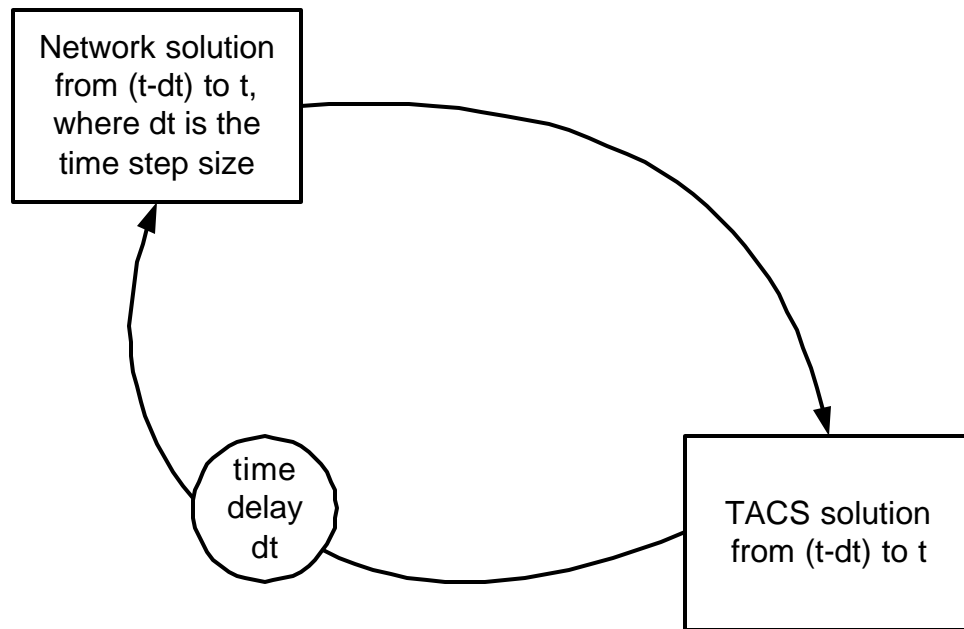


Figure 4.3 Interface between network and TACS solution [3]

MODELS is a general-purpose description language supported by an extensive set of simulation tools. It is very similar to TACS and has all the functionality of TACS. But it also allows the use of free-format, keyword-driven syntax. Also, the description of arbitrary user-defined control and circuit components is permitted. As a general-purpose programmable tool, MODELS can be used for processing simulation results either in the frequency domain or in the time domain.

Chapter 5. Cable Analysis and Modeling

5.1 Introduction

One of the choices available for NEPTUNE cable is one produced by ALCATEL. The properties of the ALCATEL cable are used for simulations described in Chapters 6 and 7. In the standard ATP cable model, the core of the cable carries the current in the forward direction, while the sheath is the return. However, the core of the ALCATEL cable is hollow and the core and sheath are in electrical contact with each other. Also, for NEPTUNE the seawater acts as the return path. To accurately model the ALCATEL cable, it is necessary to analyze the cable properties theoretically and then replicate them using the ATP model.

There are three sets of data available after cable analyses and modeling:

- 1) The cable data provided by the cable manufacturer (ALCATEL)
- 2) The cable parameters calculated using the fundamentals of transmission lines, electromagnetics and electrostatics
- 3) The ATP-computed cable parameters

These three sets of data include the values for cable resistance, cable inductance and cable capacitance. In order to have an accurate cable model, these three data sets should confirm each other.

5.2 Theoretical Calculation of Cable Inductance

5.2.1 Basic derivation for flux linkages in tubular conductors

The NEPTUNE cable has 2 conductors: the steel core (2 layers of bundled wires) and the copper sheath. Both of these conductors, as well as the insulation, are tubular. Hence a

generic formula for flux linkages associated with a tubular conductor is used to find the flux linkages for both core and sheath.

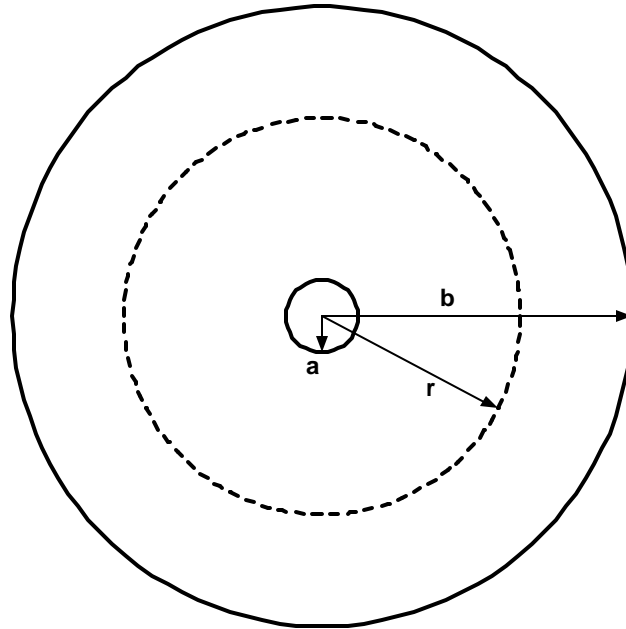


Figure 5.1 Cross-section of tubular conductor

The tubular conductor (Figure 5.1) has an inner radius a and an outer radius b . r is an arbitrary radius within the conductor.

Any current-carrying conductor has a magnetic field associated with it, which is customarily pictured in terms of lines of magnetic flux encircling the current. For an annular conductor,

$$I_T = I_i + I_e, \quad (5.1)$$

where I_T is the total flux linkage associated with the conductor, I_i is the flux linkage internal to the conductor, and I_e is the flux linkage external to the conductor.

To find flux linkage internal to the conductor, the following procedure is employed. In dc circuits, current density in the conductor is uniform. If i_r is the current enclosed by the annular element of radius r , and i is the total current enclosed by the conductor, then

$$\frac{i_r}{\mathbf{p}(r^2 - a^2)} = \frac{i}{\mathbf{p}(b^2 - a^2)}$$

$$i_r = \frac{r^2 - a^2}{b^2 - a^2} i.$$

Because the line integral of the magnetic field intensity over a closed loop is equal to the current enclosed by that loop, then

$$\oint_r H ds = i$$

For an element of radius r such that ($a < r \leq b$):

$$H \oint_r ds = \frac{r^2 - a^2}{b^2 - a^2} i$$

$$H = \frac{r^2 - a^2}{b^2 - a^2} \frac{i}{2\mathbf{p}r}$$

$$B = \mathbf{m} \frac{r^2 - a^2}{b^2 - a^2} \frac{i}{2\mathbf{p}r}$$

where \mathbf{m} is the conductor permeability and B is the magnetic flux density within the conductor.

Because the current in the conductor is uniformly distributed, the fraction of the total current enclosed within the flux line at any arbitrary radius r is given by

$$\frac{r^2 - a^2}{b^2 - a^2}.$$

The total flux at the outer radius of the conductor is:

$$\mathbf{I} = \int_a^b B \cdot da$$

$$I_i = \int_a^b \frac{r^2 - a^2}{b^2 - a^2} \mathbf{m} \frac{r^2 - a^2}{b^2 - a^2} \frac{i}{2\mathbf{p}r} dr$$

$$I_i = \frac{\mathbf{m}i}{2\mathbf{p}} \left[\frac{b^2 - 3a^2}{4(b^2 - a^2)} + \frac{a^4}{(b^2 - a^2)^2} \ln\left(\frac{b}{a}\right) \right] \quad (5.2)$$

To find the total flux linkages external to the conductor, select any annular element with radius r such that $b \leq r$. This annular element encloses the full conductor current i . Thus $i_r = i$.

$$H \oint ds = i$$

$$B = \mathbf{m}_{out} \frac{i}{2\mathbf{p}r}$$

$$H = \frac{i}{2\mathbf{p}r}$$

where \mathbf{m}_{out} is the permeability of the material external to the conductor. Assuming that c is the external radius of the material surrounding the conductor,

$$I_e = \int_b^c \mathbf{m}_{out} \frac{i}{2\mathbf{p}r} dr$$

$$I_e = \frac{\mathbf{m}_{out}i}{2\mathbf{p}} \ln\left(\frac{c}{b}\right) \quad (5.3)$$

This is the flux linkage external to the tubular conductor.

5.2.2 Inductance of ALCATEL cable

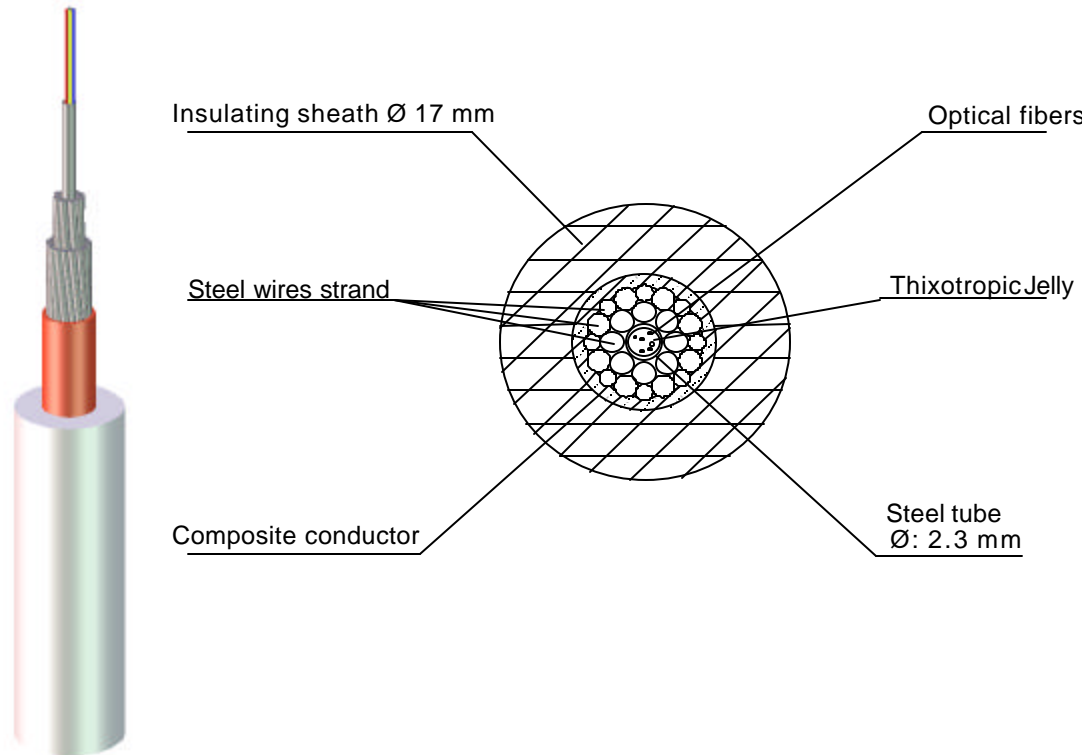


Figure 5.2 Proposed cable for the NEPTUNE observatory

The OALC-4 ALCATEL cable consists of a central hollow steel tube, which carries the optic fibers (Figure 5.2). This steel tube is surrounded by steel strands, which act as a core. The core is surrounded by a copper sheath. The steel strands and the copper sheath form a composite conductor that is enclosed by a polyethylene insulator.

The flux linkages associated with the cable are the sum of the flux linkages due to the core current and the flux linkages due to the sheath current.

5.2.2.1 Flux linkages of core

Let I_{steel} be the sum of the flux linkages due the core current in all 3 regions of core (steel), sheath (copper), and insulator (polyethylene).

Substituting equations (5.2) and (5.3) into equation (5.1),

$$I_{steel} = \frac{\mathbf{m}_{st} i_{st}}{2\mathbf{p}} \left[\frac{b^2 - 3a^2}{4(b^2 - a^2)} + \frac{a^4}{(b^2 - a^2)^2} \ln(b/a) \right] + \frac{\mathbf{m}_{cu} i_{st}}{2\mathbf{p}} \ln(c/b) + \frac{\mathbf{m}_{ns} i_{st}}{2\mathbf{p}} \ln(d/c) \quad (5.4)$$

where i_{st} is the current in the core, \mathbf{m}_{st} is the permeability of the steel, \mathbf{m}_{cu} is the permeability of the copper, and \mathbf{m}_{ns} is the permeability of the insulator. Also, a is the inner radius of the steel core, b is the outer radius of the steel core and inner radius of the copper sheath, c is the outer radius of the copper sheath and inner radius of the insulator, while d is the outer radius of the insulator.

5.2.2.2 Flux linkages of sheath

Let I_{cu} be the sum of the flux linkages due the sheath current in two regions of sheath and insulator. Substituting equations (5.2) and (5.3) into equation (5.1),

$$I_{cu} = \frac{\mathbf{m}_{cu} i_{cu}}{2\mathbf{p}} \left[\frac{c^2 - 3b^2}{4(c^2 - b^2)} + \frac{b^4}{(c^2 - b^2)^2} \ln(c/b) \right] + \frac{\mathbf{m}_{ns} i_{cu}}{2\mathbf{p}} \ln(d/c) \quad (5.5)$$

where i_{cu} is the current in sheath.

Note that in equation (5.5) I_{cu} does not have a term relating to the flux linkages within the core. This is because the sheath current enclosed by any annular element within the core is zero.

The total flux linkages associated with the cable are given by:

$$I_{cable} = I_{st} + I_{cu}.$$

Using the physical dimensions of the cable provided by ALCATEL,

$$a = 0.00115 \text{ m}$$

$$b = 0.0036 \text{ m}$$

$$c = 0.00416 \text{ m}$$

$$d = 0.0085 \text{ m}$$

I_{cable} is computed using equation (5.5).

$$I_{cable} = 2.1081 * 10^{-6} i_{st} + 8.9849 * 10^{-9} i_{cu} \quad (5.6)$$

Because, $i_{cable} = i_{st} + i_{cu}$ the current distribution within the core and sheath is computed as,

$$R_{st} i_{st} + j \omega L_{st} i_{st} = R_{cu} i_{cu} + j \omega L_{cu} i_{cu}, \quad (5.7)$$

where the left side of equation (5.7) is the voltage drop per unit length of the steel core, while the right side is the voltage drop per unit length of the copper sheath.

Because, $L i = I$,

$$R_{st} i_{st} + j \omega L_{st} i_{st} = R_{cu} i_{cu} + j \omega L_{cu} i_{cu}$$

$$R_{st} = \frac{r_{st}}{p(b^2 - a^2)} = 5.607 * 10^{-3} \Omega/m$$

$$R_{cu} = \frac{r_{cu}}{p(c^2 - b^2)} = 1.263 * 10^{-3} \Omega/m.$$

r_{st} and r_{cu} are the resistivities of the steel core and the copper sheath materials respectively.

For dc conditions, $\omega = 0$. Solving equation (5.7), yields,

$$i_{st} = 0.1838 * i_{cable} \quad (5.8)$$

$$i_{cu} = 0.8162 * i_{cable}. \quad (5.9)$$

Substituting equations (5.8) and (5.9) in equation (5.6),

$$\begin{aligned} \mathbf{I}_{cable} &= (3.874*10^{-7}) i_{cable} + (7.333*10^{-9}) i_{cable} \\ \mathbf{I}_{cable} &= (3.947*10^{-7}) i_{cable}. \end{aligned} \quad (5.10)$$

Thus the composite inductance of the cable is,

$$L = \frac{\mathbf{I}_{cable}}{i_{cable}}.$$

$$L = 0.3947 \mu\text{H/m}$$

5.3 Calculation of Capacitance

The cable capacitance per unit length can be calculated by the formula:

$$C = \frac{2pe}{\ln\left(\frac{d}{c}\right)} \text{ F/m}, \quad (5.11)$$

where e is the permittivity of the insulator, d is the outer radius, and c is the inner radius of the insulator.

For the ALCATEL cable these constants are:

$$\epsilon = \epsilon_0 \epsilon_R = (2.3)*(8.854*10^{-12})$$

$$d = 0.0085 \text{ m}$$

$$c = 0.00416 \text{ m}$$

Substituting these constants in equation (5.11) yields,

$$C = 0.179 \text{ nF/m}.$$

5.4 Computation of Cable Parameters by ATP

The *Cable Constants/ Cable Parameters* in ATP [10] generate all the data required for the line and cable models. The *Cable Constants/ Cable Parameters* routines use generic algorithms like Carson's formula [10] to calculate the parameters of the line or cable. The two most important parameters for the frequency-dependent models are the characteristic impedance and the propagation constant as a function of frequency.

For a cable model, the *Cable Constants/ Cable Parameters* routines require information about the cable such as the number of cables, their lengths and physical dimensions. Information such as cable structure of core, sheath, armor and insulation along with their resistivities, permittivities and permeabilities is needed. The characteristics of the ground is also relevant.

The proposed NEPTUNE cable has the core and sheath connected, thus electrically, they can be considered as two parallel conductors. However, the *Cable Constants/ Cable Parameters* routine in ATP treats the core and sheath of the cable as forward and return conductors.

Modeling the cable with a separate core and sheath gives erroneous results. The high resistivity and high permeability of the cable core, combined with the problem that the cable core was carrying the entire forward cable current, would result in the large values of both cable inductance and cable resistance. To resolve this problem, the cable core and sheath are treated as a composite conductor. The critical parameters in modeling the composite conductor are the composite resistivity (r_{comp}) and the composite permeability (m_{comp}).

5.4.1 Calculation of r_{comp}

The steel core and the copper sheath are conductors in parallel. Their currents will be distributed depending on their resistances.

$$R_{comp} = R_{st} \parallel R_{cu}$$

$$\frac{r_{comp}}{\rho(c^2 - a^2)} = \frac{\frac{r_{st}}{\rho(b^2 - a^2)}}{\frac{r_{st}}{\rho(b^2 - a^2)} + \frac{r_{cu}}{\rho(c^2 - b^2)}}$$

Using the physical parameters of the cable mentioned in Section 5.2.2,

$$r_{comp} = 5.1753 * 10^{-8} \text{ Wm.}$$

5.4.2 Calculation of m_{comp}

The flux linkages associated with the cable are given by,

$$I_{cable} = I_{st} + I_{cu} = I_{comp}.$$

The flux linkages associated with the composite conductor current encircling the internal conductor, and the insulator can be computed using equations (5.2) and (5.3),

$$I_{comp} = \frac{m_{comp} * i_{cable}}{2\rho} \left[\frac{c^2 - 3a^2}{4(c^2 - a^2)} + \frac{a^4}{(c^2 - a^2)^2} * \ln(c/a) \right] + \frac{m_{ns} * i_{cable}}{2\rho} \ln(d/c)$$

$$I_{comp} = 4.348 * 10^{-8} * m_{comp} * i_{cable} . \quad (5.12)$$

Using the physical parameters of the cable (Section 5.2.2),

$$m_{comp} = 9.0788$$

yielding the relative permeability of the composite conductor.

Using these values of resistivity and permeability in the ATP model for the composite conductor we obtain the results for the cable parameters shown in Table 5-1.

Table 5-1 Comparison of cable parameter values

	Theoretical values	ATP values	Manufacturer values
R (Ω/km)	1.03	1.03	1.0
L (mH/km)	0.3947	0.3948	0.4
C ($\mu\text{F}/\text{km}$)	0.179	0.179	0.2

5.5 Computation of Ground Parameters

To calculate the internal impedance of any tubular conductor, ATP uses the generalized formula for tubular conductors:

$$Z_{tube-in} = \frac{\mathbf{r}m}{2pqD} \left[I_0(mq) K_1(mr) + K_0(mq) I_1(mr) \right] \frac{\Omega}{m}, \quad (5.13)$$

where $Z_{tube-in}$ is the internal impedance of tubular conductor, \mathbf{r} is the resistivity of earth, q is the inner radius of the tubular conductor, and r is the outer radius of the tubular conductor. I and K are the modified Bessel functions of the first and second kind [16], and m is the reciprocal of the complex depth of penetration.

$$m = \sqrt{\frac{j\mathbf{v}\mathbf{m}}{\mathbf{r}}},$$

where \mathbf{m} is the permeability of earth, and

$$D = \left[I_1(mr) K_1(mq) - K_1(mr) I_1(mq) \right].$$

Applying this generalized formula for the earth-return impedance, the outer radius r is set to infinity, and $q = d$. Hence,

$$Z_{earth} = \frac{rm}{2pR} * \frac{K_0(mr)}{K_1(md)}, \quad (5.14)$$

where d is the outside radius of the tubular conductor and insulation.

For NEPTUNE cable and for most submarine cables, the seawater has a resistivity $r = 0.2\Omega\text{m}$ at constant temperature. Also, the relative permeability of seawater is given by $m_{sea} = 1$.

ATP calculation of the ground impedance provides the following values:

$$R = 1.30698 * 10^{-7} \Omega/\text{m} = 0.130698 \text{ m}\Omega/\text{km}.$$

$$X = 1.44254 * 10^{-6} \Omega/\text{m} @ \text{freq.} = 0.1\text{hz}.$$

Hence,

$$L = 2.2958 \text{ mH/km}.$$

We need to know whether these ATP-computed values match with the actual values. Equation (5.14) can be simplified under some assumptions, as suggested by Bianchi and Luoni [17]. They suggest that

$$\frac{|m|D_i}{2} \ll 1,$$

where D_i is the outer diameter of the cable.

In equation (5.14) $K_0(x)$ and $K_1(x)$ can be replaced by their asymptotic expansions for very small values of x leading to,

$$Z_{sea} = \frac{wm}{8} + jw \frac{m}{2p} \ln(2R_e/D_i). \quad (5.15)$$

Substituting the following,

$$\begin{aligned} |m| &= 1.9869 * 10^{-3} \\ \frac{D_i}{2} &= d = 0.0085\text{m} \end{aligned}$$

we verify that

$$\frac{|m|D_i}{2} \ll 1.$$

Now solving equation (5.15) at frequency of 0.1Hz,

$$R = 0.098 \text{ m}\Omega/\text{km}$$

$$L = 2.221 \text{ mH/km.}$$

Table 5-2 gives a comparison of the ground parameters computed by ATP and the ones obtained by theoretical calculations. These two results agree well with each other.

Table 5-2 Comparison of ground parameter values

	Theoretical values	ATP values
R (mΩ/km)	0.098	0.131
L (mH/km)	2.221	2.295

Chapter 6. EMTP Models for Restrikes and Shore Station Control

6.1 Introduction

In Version 1 local intelligence and sensors control the operation of the sectionalizing switches. The details of the switching actions for Version 1 are described in Chapter 2. A fault in the power system causes overcurrents in the backbone. The nearest nodes sense these overcurrents and the node controller initiates the control actions, which will open the backbone circuit breaker.

In Version 2 a fault causes the system to enter the *fault* mode of operation, as described in Chapter 3. Here again, the nearest nodes sense overcurrent. However, they do not respond to the fault in any way. The response to the fault is at the system level by the shore station controls. The branching units and nodes, which are close to the fault, must then withstand the overcurrent until the shore station responds.

EMTP simulations, which take into consideration arcing and restrikes, play an important role in component design. Electronics designed with the aid of these simulations have a better chance of surviving the dynamic conditions in the real power system.

A simplifying assumption for carrying out the EMTP simulations for the faulted condition is to assume the shore station supply as a voltage source that supplies infinite current. This also represents a worst-case scenario. A conservative approach is to maintain this assumption and then design the system electronics. If the electronics are able to withstand transients under this assumption, they are more likely to survive under actual operating conditions.

However, in the NEPTUNE power system, the shore station supply will have current-limiting capabilities. If the current exceeds a certain threshold, the control circuitry within the shore power supply responds. The control circuitry reduces the shore voltage, which

in turn limits the current. Strategies to implement this current-limiting feature and to model it in EMTP are discussed in this chapter.

6.2 Initial Switching Arcs

Mechanical switches are the most commonly used circuit breakers. The mechanical switch has two contacts that connect two sections of the circuit. During the process of circuit interruption, these contacts part. When the fault is interrupted the current through the circuit breaker is high, which results in a very high current density at the contacts surface area. This can cause the contact material to overheat. In addition, there is rapid ionization of the dielectric separating the contacts. This is known as the *switching arc*.

The switching arc is sustained in the circuit breaker for a short period, which depends upon the type of switch used and the magnitude of the interrupted current. The arc resistance, which is very small initially, gradually builds up until the arc resistance is so large that the arc can no longer be sustained.

Repeated interruption of high currents degrades the performance of the circuit breaker. Therefore, it is necessary to use switches, which minimize the arcing effects. This is the reason the vacuum switch is the preferred choice for NEPTUNE. Because, the contacts of a vacuum switch are separated in vacuum, there is no media for the process of ionization, and thus the arcing effects are minimized, but not eliminated.

In case of the NEPTUNE circuit breaker, initial arcing cannot be completely prevented by any circuit design. The initial arc produced by the interruption of dc current in Version 1 is unavoidable. However, some vacuum switch manufacturers have developed switch structures that minimize arcing. Further, these advanced switch structures are qualified to withstand multiple arcings.

An arc model would represent the arc as a time-dependent, non-linear resistance. EMTP simulations for this work do not model the initial arc. Here, the simulations consider the switch closed during arcing. At the end of the arcing interval, the switch is opened.

6.3 Restrikes

Restrike is another phenomenon that may occur while the circuit breaker is opening. As the breaker's electrodes separate, the dielectric medium of the circuit breaker begins to regain its strength. The *withstanding voltage* of the breaker is the maximum voltage that the breaker can withstand across its terminals, without arcing. When the breaker opens, its withstanding voltage increases linearly. At the same time, the voltage across the contacts builds up in accordance with the nature of the switching event and the system characteristics. If the voltage buildup exceeds the withstanding voltage at any instance, an interelectrode breakdown occurs and arc current is produced; this is known as restrike.

Figure 6.1 illustrates the restrike where the withstanding voltage is assumed to increase linearly to the insulation level of the breaker. In case 1, the voltage buildup across the contacts never exceeds the withstanding voltage of the breaker, thus restrike does not occur. In case 2, the voltage buildup exceeds the withstanding voltage at time t_s , and restrike occurs. In the event of restrikes, excessive overvoltage and high dv/dt is produced. These transients have the potential to damage the loads, cable and equipment.

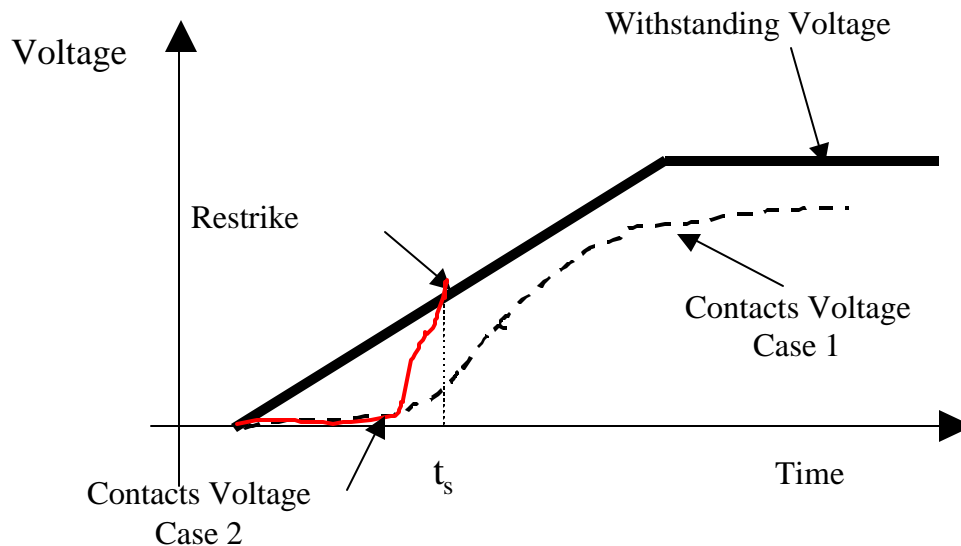


Figure 6.1 Restrikes in a circuit breaker

To eliminate restrikes in Version 1, the dc breaker configuration in Figure 2.4 is proposed. The full description of the breaker configuration and operation is given in Chapter 2. The selection of the breaker's components should be made to ensure that the withstanding voltage is always higher than the voltage buildup across the breaker. Two components in this circuit must be carefully selected to prevent restrikes: the vacuum interrupter (S3), which is the first switch to open; and the bypass capacitor (C). The bypass capacitor controls the voltage across the vacuum interrupter during the opening process. The vacuum interrupter should be as fast as possible to allow for rapid recovery of its withstanding voltage. Faster switches demand smaller bypass capacitors.

6.3.1 Modeling of restrikes

In this study, restrikes are modeled as a voltage-dependent switch. The algorithm for the restrike model operates as follows:

- 1) The withstanding voltage is modeled as a ramp function with its slope equal to the maximum withstanding voltage divided by the travel time of the interrupter.
- 2) After the main interrupter (S3 in Figure 2.4) is opened, the *initial arcing* is allowed for some time. This time is dependant both on the maximum withstanding voltage of the switch and its travel time.
- 3) After this time the arc resistance becomes large enough and the initial arc is extinguished.
- 4) Then S3 interrupts the current and the capacitor C is charged. The voltage across the capacitor is observed.
- 5) If the capacitor voltage exceeds the withstanding voltage of the switch, S3 is reclosed, simulating a restrike.

The restrike model is developed using the MODELS feature in ATP.

6.3.2 Selection of capacitor and vacuum switch in Version 1

The prevention of restrikes depends on three parameters: 1) the capacitor size, 2) the speed of the vacuum interrupter (travel time), and 3) the maximum withstanding voltage of the vacuum interrupter.

If the capacitor value is sufficiently large, the voltage buildup across the breaker may not be fast enough to exceed the withstanding voltage of the vacuum interrupter. Thus, restrikes can be prevented. However, a large capacitor will be larger physically, and cost more.

While a small value capacitor is smaller in size and costs less, the voltage buildup across it will be faster and is more likely to exceed the withstanding voltage of the vacuum switch, resulting in restrikes.

The maximum withstanding voltage and travel time of the vacuum interrupter determine the slope at which the withstanding voltage increases. If the slope is shallow with respect to the voltage buildup of the capacitor, restrikes will occur.

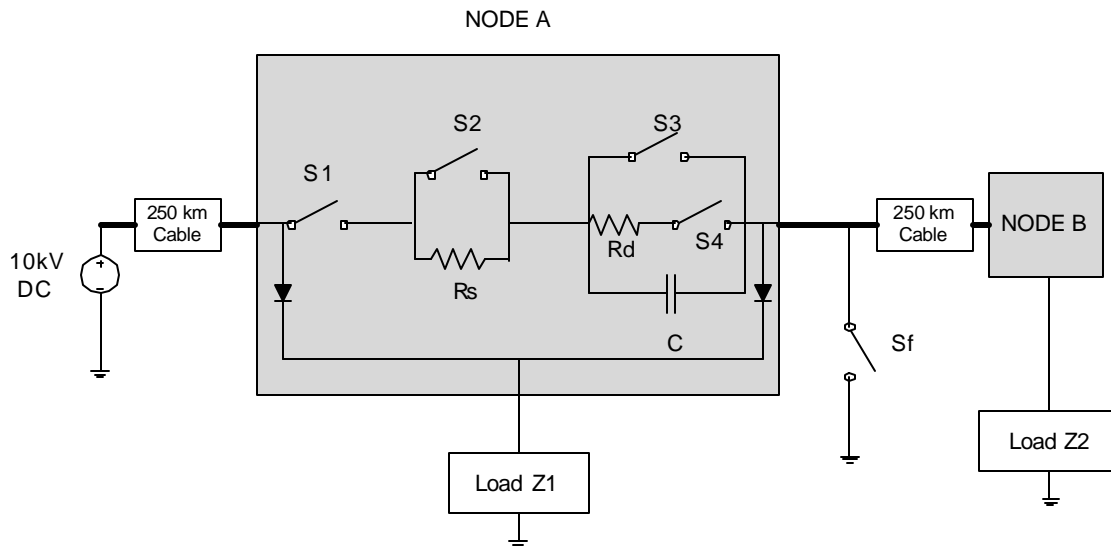


Figure 6.2 Simulation circuit for restrike model

To determine the proper value of the capacitance, a study was carried out based on the circuit in Figure 6.2. The chosen cable section was 250 km in length between the breaker and the shore station. It was also assumed that the distance between Node A and Node B was 250 km. Z2 represents the load of node B and switch Sf was used to simulate faults. The load Z1 was a 1 k Ω resistive. As a result, the cable current at the shore station side was higher than the expected normal operation.

Table 6-1 shows the summary of the simulation results. The various speeds and maximum withstanding voltages were selected based on the market availability of vacuum interrupters. The table also shows the minimum capacitance required to prevent restrikes.

The simulations were performed for successive integer values of capacitance, starting from an arbitrary low value. The minimum capacitance that did not produce a restrike is given in the table.

Table 6-1 Restrike studies

Maximum voltage across switch	Travel time of switch	Minimum value of capacitor to prevent restrikes (μF)
15 kV	5 ms	2
15 kV	10ms	5
15 kV	18 ms	10
25 kV	15 ms	1
25 kV	18 ms	1
25 kV	20 ms	1

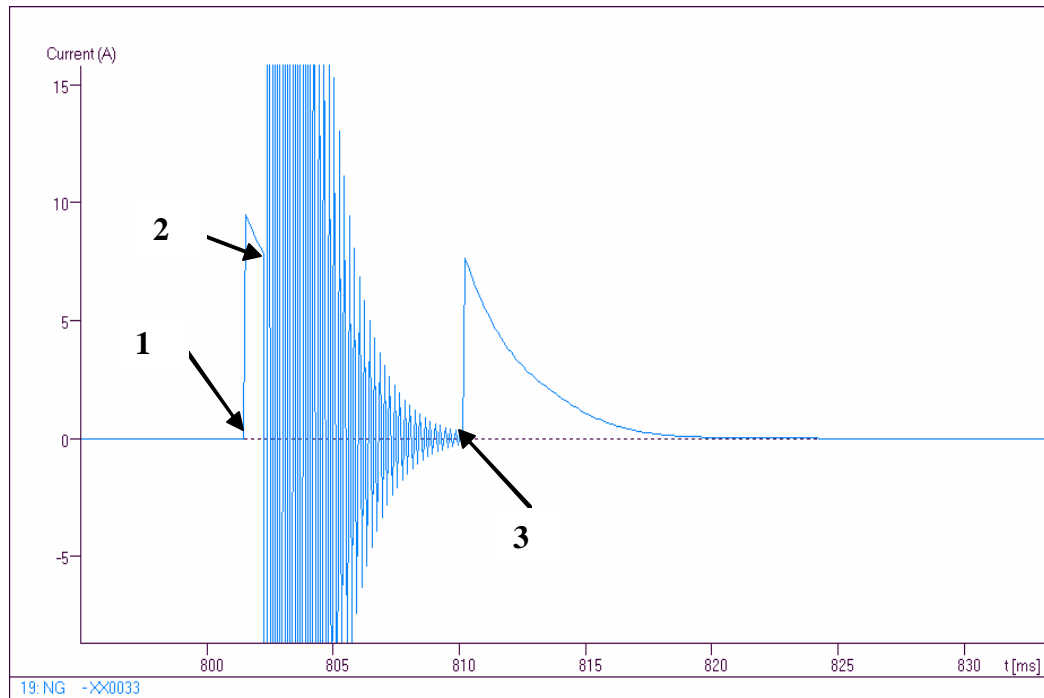


Figure 6.3 Current through capacitor with restrikes when $C=4\text{mF}$

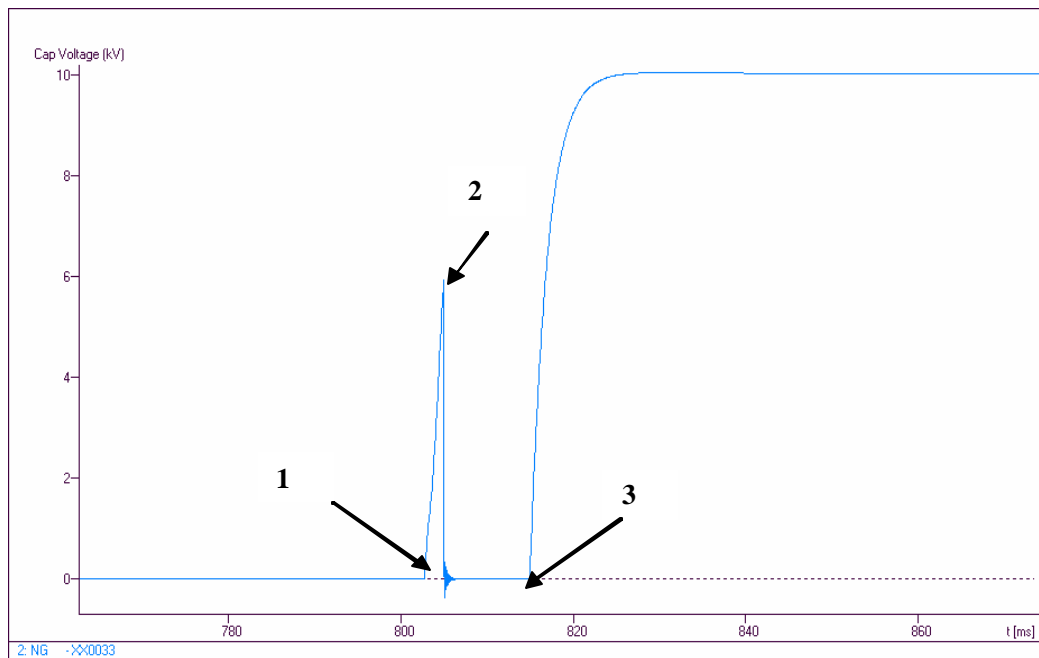


Figure 6.4 Voltage across capacitor for $C=4\text{mF}$

Figure 6.3 and Figure 6.4 show the capacitor current and the voltage across the main switch (which is also the capacitor voltage), respectively. In this simulation, the vacuum switch is assumed to have a maximum withstanding voltage of 15 kV and a traveling time of 10 ms. A bypass capacitor of 4 μF was used for these simulations.

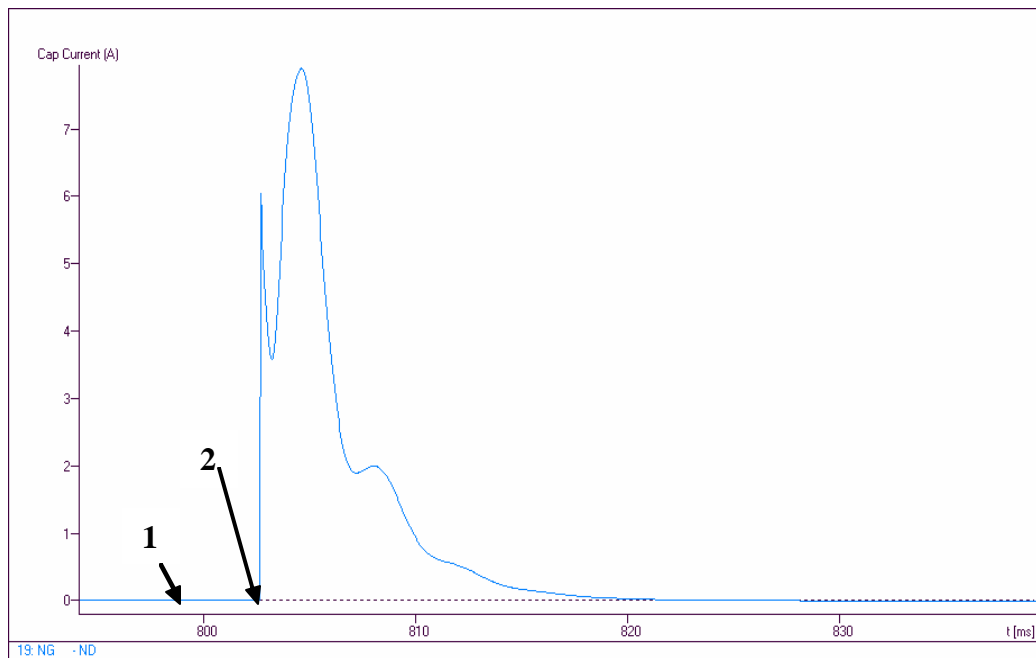


Figure 6.5 Capacitor current without restrikes when $C=5 \text{ mF}$

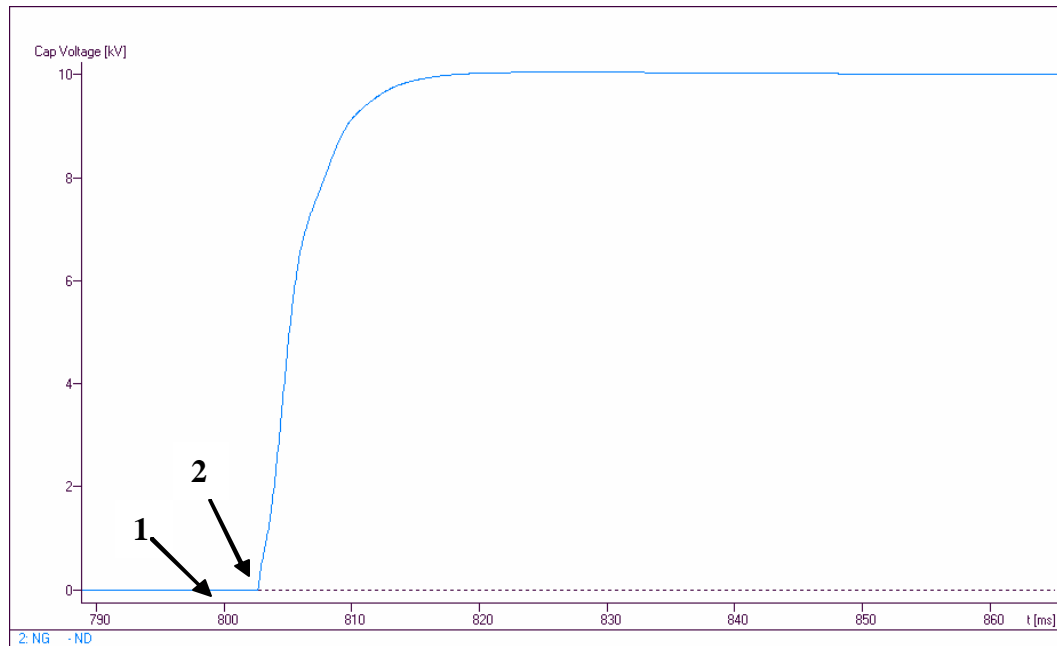


Figure 6.6 Voltage across capacitor for $C=5 \text{ mF}$

At 800 ms when switch S3 is opened, the initial arcing is extinguished at point 1 (Figure 6.3 and Figure 6.4). Next, the capacitor starts charging, and at point 2 a restriking occurs. The restriking arc lasts for about 10 ms, after which the arc is assumed to be extinguished at point 3. Between 2 and 3, the capacitor current oscillates at high frequencies.

The second case (Figure 6.5 and Figure 6.6) uses a larger capacitance ($5 \mu\text{F}$). No restriking occurs and the opening of the capacitor is successful.

It should be noted that this simulation was carried out for a node 250 km from the source. For nodes closer to the source, the capacitor must be larger in size to prevent restriking.

6.4 Modeling of Shore Station Power Supply Controls

Power supplies situated at the two shore stations energize the NEPTUNE power system. One of the shore stations is located near Victoria, B.C., while the other is at Nedonna Beach, OR. Each of the shore power supply has a power rating of 100kW, 10kV dc.

The fiber optic communication system supported by NEPTUNE requires *repeaters* located at fixed distances in order to maintain the quality and amplitude of the optical signal. These optical repeaters cannot withstand more than a 10A steady-state current. Thus it is necessary to limit the current in the backbone to less than 10A.

The current in the network can increase above 10A due to a variety of reasons. Load fluctuations, topology changes, and low impedance faults are some of the typical ways this can occur. Whenever the cable current at the shore station exceeds the pre-defined value of 10A, the control circuitry initiates a control action to limit the current.

The actual design of the current limiting circuitry is based on a feedback loop. An increase in current at the output of the shore station converter (power supply) is fed back to the input. The input controls react to this by reducing the output voltage such that the output current is maintained at approximately 10A.

The design of the power system components is generally based upon worst-case assumptions. An infinite current, voltage source will allow a short circuit fault to draw large amounts of current. The design of the capacitor and vacuum switch in the previous section is based upon this worst-case assumption. In reality this shore station current limiting capability will limit the current in case of a short circuit fault. The capacitors and vacuum switches designed as per the previous section will definitely survive under actual conditions, as they will be subjected to lower thermal stresses.

To study the behavior of the power network under actual operating conditions, it is necessary to model the shore station current limiting capability. An EMTP model was developed for this purpose using MODELS.

6.4.1 Model 1

The shore station controls maintain the steady-state current to 10A, and should not react to transient overcurrents. Such transient overcurrents die out quickly and any control action to limit this overcurrent is unnecessary. The control action to limit overcurrent results in a reduction in output voltage and because the current transients will subside quickly, this control action results in inefficient system operation.

The operating steps for this shore station current limiting model are:

- 1) Monitor the output current of the power supply.
- 2) At each time step, calculate the average current over the past 5ms. This step prevents a current transient from initiating a control action.
- 3) If the average is exceeding a pre-defined limit (e.g., 10A), start the current limiting procedure.
- 4) The current limiting procedure involves disconnecting the original voltage source and connecting a TACS voltage source.
- 5) The TACS voltage source will have a final value so that the output current is restricted to the pre-defined limit.
- 6) The value of the TACS voltage source is gradually reduced from its original value of 10kV to its final value over discrete time steps of 25ms.
- 7) If the fault causing the overcurrent is removed from the circuit, the average begins to drop at each time step. The value of the TACS voltage source is then raised gradually over discrete time steps.
- 8) When the TACS source value reaches 10kV it is disconnected and the original 10kV voltage source is reconnected.

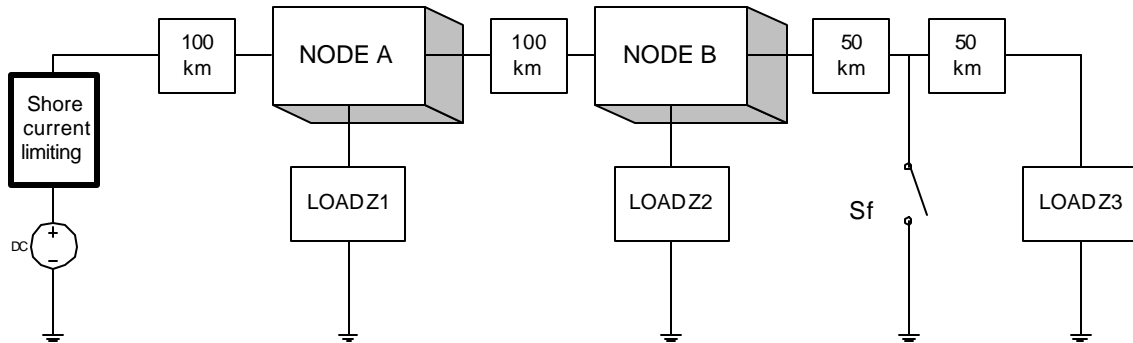


Figure 6.7 Simulation circuit for shore station current limiting model

Figure 6.7 shows the simulation circuit used to demonstrate the model for the shore station current limiting process for Version 1. (For circuit configuration see Figure 2.4). These two nodes are separated by 100km of cable and also 100km between the first node and the shore. The switch Sf, 50km from Node B, simulates the fault. The fault is initiated at the time $t = 1.0s$ in the simulation and is cleared at time $t = 3.0s$.

Figure 6.8 and Figure 6.9 show the current and voltage at the output of the power supply. Point 1 shows the pre-fault conditions, where the voltage is 10kV and the current is below 10A. At the 1.0s mark, the fault occurs and a large current is drawn from the source. The shore current limiting is then activated. As point 2 shows, the voltage is gradually reduced in increments and this causes the current to reduce and finally stabilize at 10A. At the 3.0s mark the fault is cleared. This causes a reverse action (point 3) and the voltage is gradually raised back to its initial 10kV value.

It should be noted that the given simulation does not reflect the actual time response of the shore station current-limiting circuitry. This simulation simply provides an overview of the likely concept to be used.

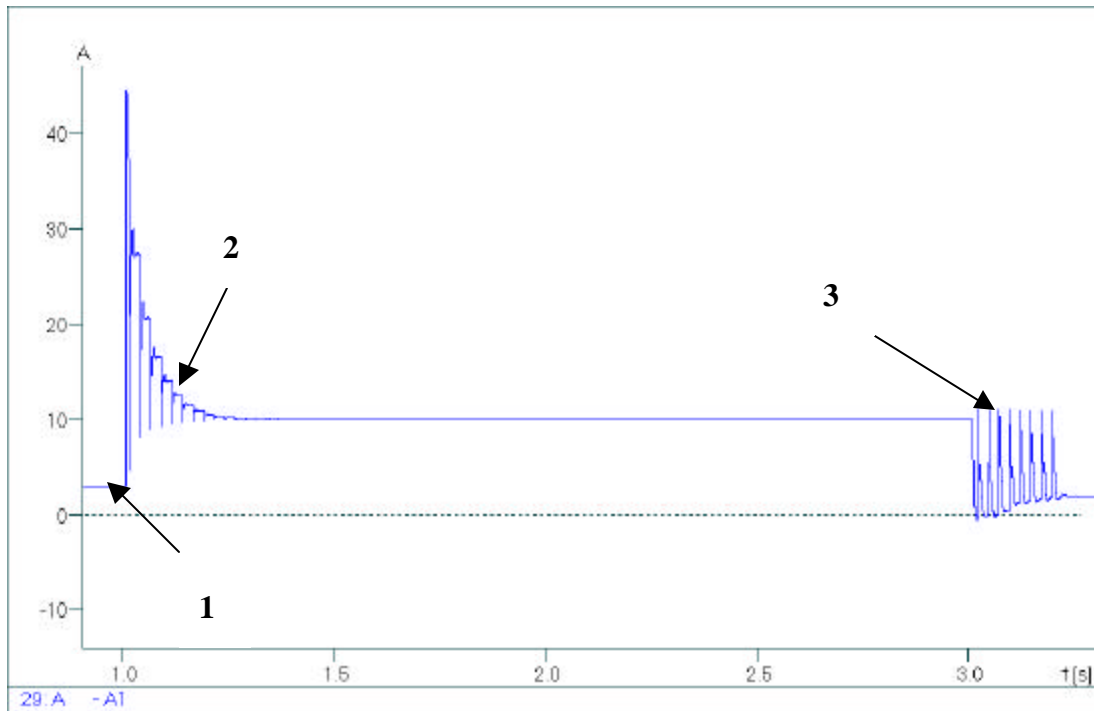


Figure 6.8 Output current of shore power supply during current limiting

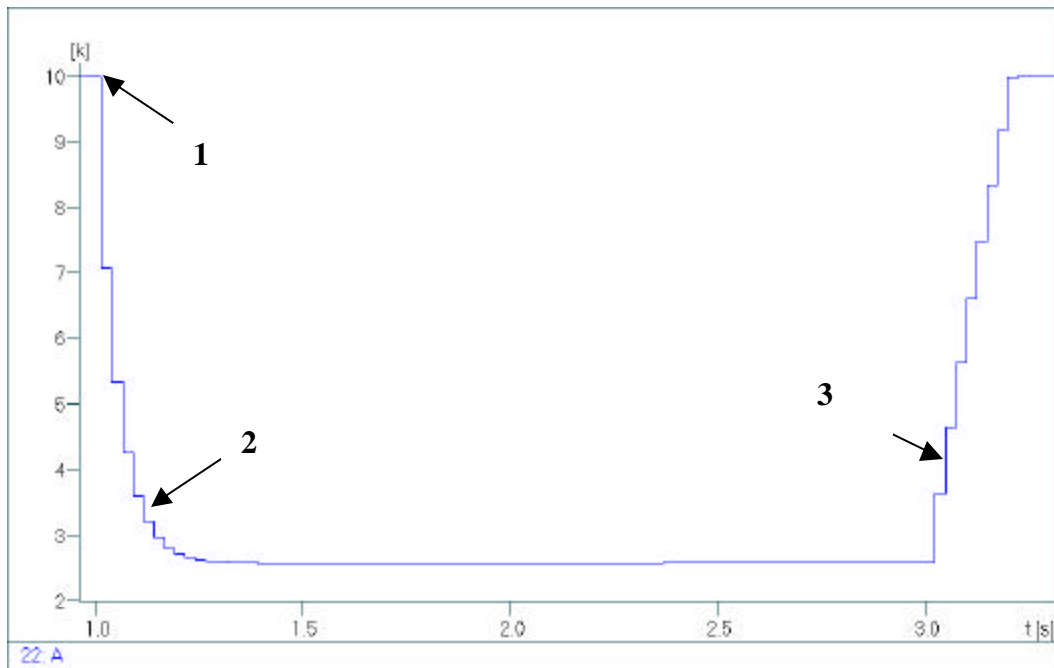


Figure 6.9 Output voltage of shore power supply during current limiting



Figure 6.10 Output current of shore power supply without current limiting

Figure 6.10 shows the output current of the power supply when no current limiting algorithm is imposed. The simulation circuit used is the same as in Figure 6.7. The fault occurs at the 1.0s mark and a large current is drawn from the source. The shore voltage remains at 10kV dc.

Chapter 7. Network Transient Simulations

7.1 Introduction

It is important to simulate the transient behavior of the power system under different operating scenarios and different contingencies. This chapter details the description and results of such EMTP simulations.

To identify system stress, it is useful to study processes such as the opening of the circuit breaker, the closing of the circuit breaker, and the inrush currents. In Version 1, the nearest nodes respond to the fault by opening the circuit breaker and interrupting the fault current. Transients created in such situations are more severe when the fault is located close to the shore station. In Version 2 the shore station controls respond to a fault by interrupting the power supplies. Placement of the pre-insertion resistance is studied by performing simulations.

All simulations in this chapter examine the behavior of particular sections of the network. The entire network model is unnecessary, as the idea is to simulate worst-case conditions for the transient response of the system.

7.2 Version 1: Simulation of Non-Fault System Operation

Figure 7.1 shows the arrangement of the simulated circuit. There are four nodes with a shore station supply on either side of the cascaded network section. Each node has a breaker circuit as described in Figure 2.4.

The waveforms at Node 3 are shown for this study. Node 3 is a central node that is representative of most NEPTUNE nodes. Node 3 is 200 km from the nearest shore station and 300 km from the distant shore station.

The switching sequence of the node breakers is shown in Figure 7.2. A *high* represents a closed circuit breaker and a *low* represents an open circuit breaker. The load of each node is assumed to be $10\text{ k}\Omega$, the bypass capacitor of the breaker is $5\text{ }\mu\text{f}$, and the soft starting resistance is $1\text{ k}\Omega$.

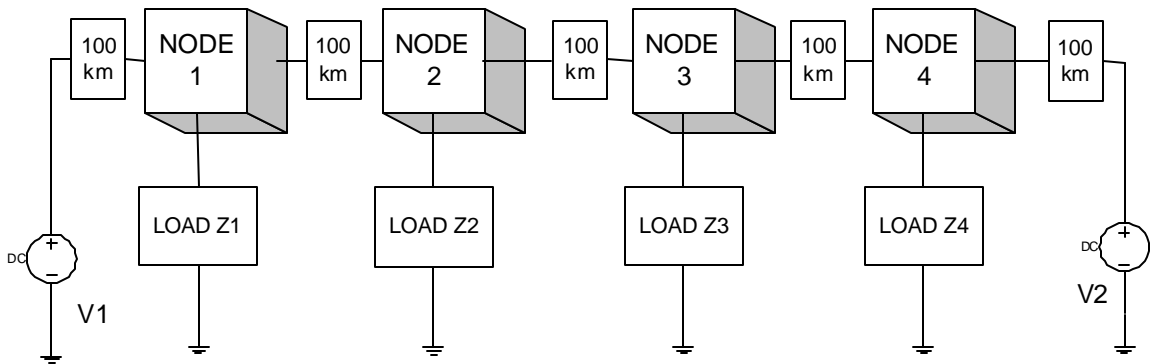


Figure 7.1 Steady-state simulation circuit

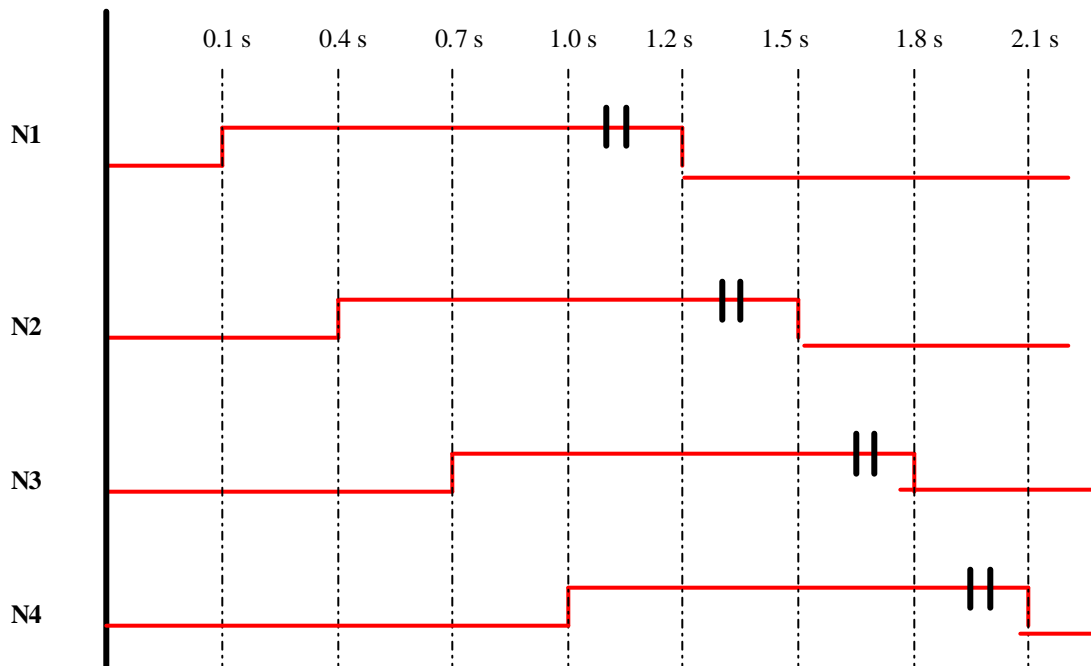


Figure 7.2 Time sequence of node breaker switching

Figure 7.3 and Figure 7.4 show the current and voltage waveforms at the left end of node 3. The current begins to flow through the left diode of Node 3, and the voltage rises at 400 ms when the breaker in Node 2 closes. At 700 ms, the breaker switches in Node 3 start their closing sequence. The current spike that occurs at this time is due to the closing of S1 and S3 and opening of S2 in the breaker of Node 3. The voltage drops slightly due to the energization of the cable through the soft-closing resistor. At 750 ms the soft-closing resistor is removed from the circuit by closing S2. After this switching action, the current through the node stabilizes at its steady-state value.

At 1.0 s Node 4 closes and the current at Node 3 drops because the loads of Nodes 3 and 4 are fed from shore station 2. The current drawn from shore station 1 into Node 3 is near zero.

At 1.2 s Node 1 opens and all the loads are fed by shore station V2 (Figure 7.1). The negative current implies a reverse in the current flow. At 1.8 s Node 4 opens and Node 3 is isolated from both shore stations.

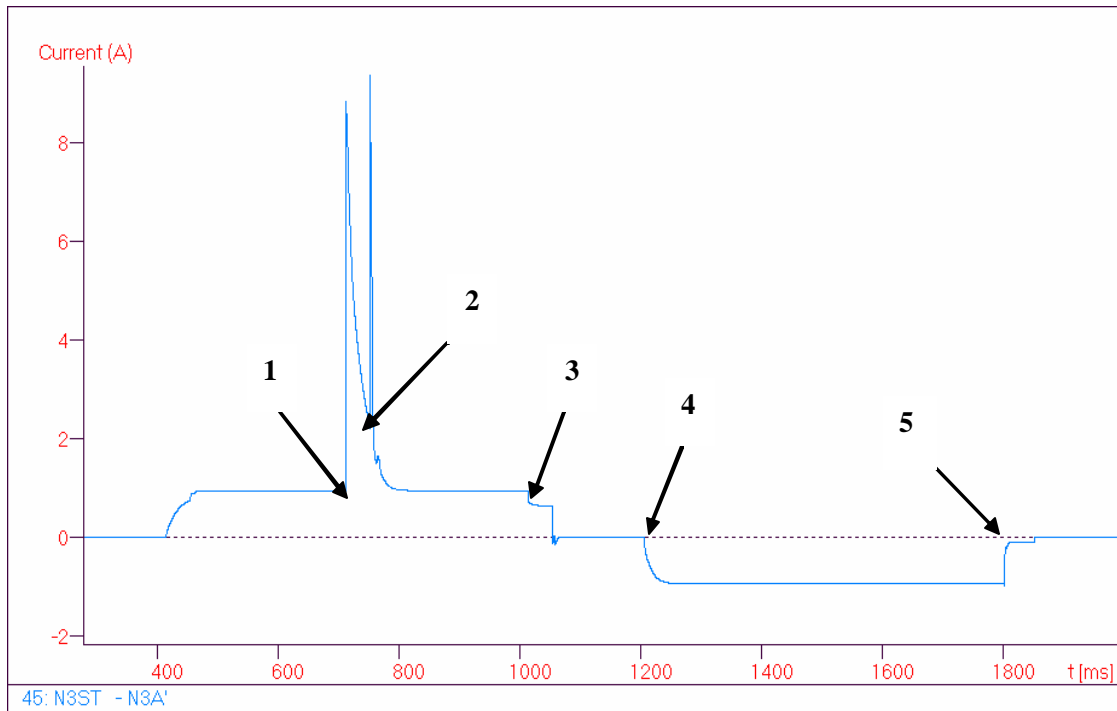


Figure 7.3 Current at the left input of Node 3

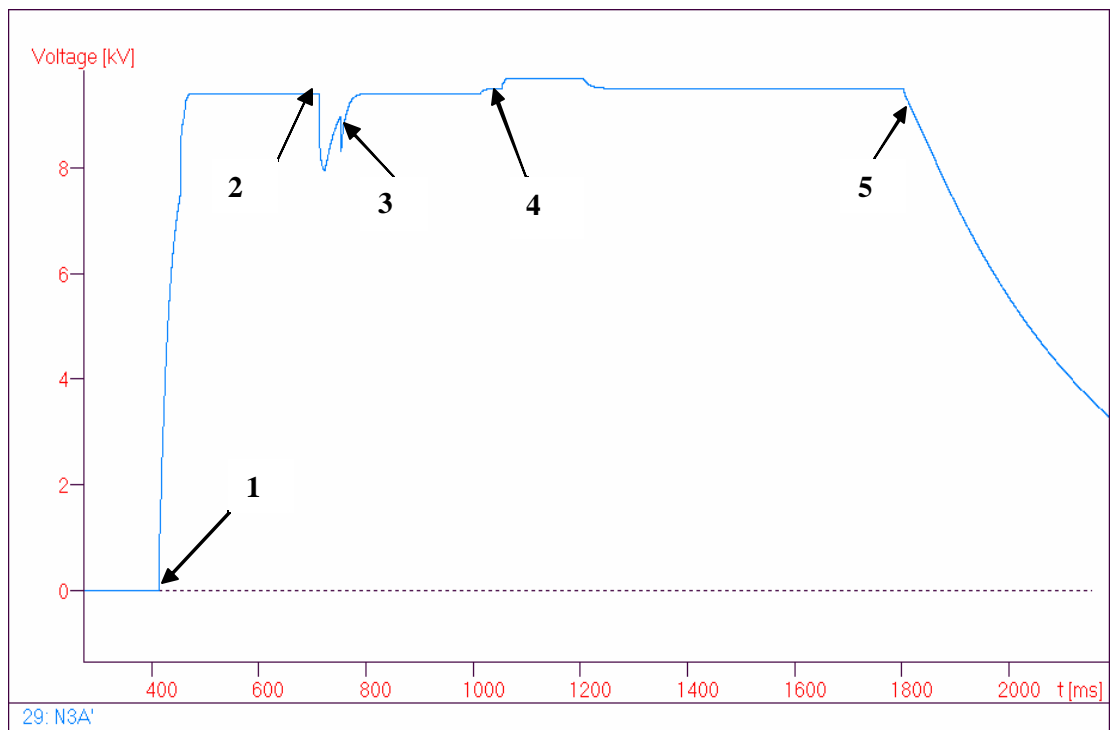


Figure 7.4 Voltage at the left input of Node 3

The voltage and current of the left diode in Node 3 are shown in Figure 7.5 and Figure 7.6. After 400 ms the breaker at Node 2 closes and the diode becomes forward-biased. The first shore station through this diode feeds the load connected to Node 3. At 700 ms the breaker in Node 3 closes and current fluctuation in the diode results from voltage fluctuation. At 1.8 s the breaker at Node 3 opens, leading to the commutation of the left diode. The shore station V2 through the right diode feeds the load of Node 3. The exponential increase in the voltage waveform across the left diode is due to the cable capacitance between Node 2 and Node 3.

At 2.1s the breaker at Node 4 opens and the load at Node 3 no longer connects to a supply, which causes the voltage drop across the left diode of Node 3 to gradually reduce to zero (due to the cable capacitance). The negative spike in Figure 7.6 is due to a numerical error with diode switching in ATP.

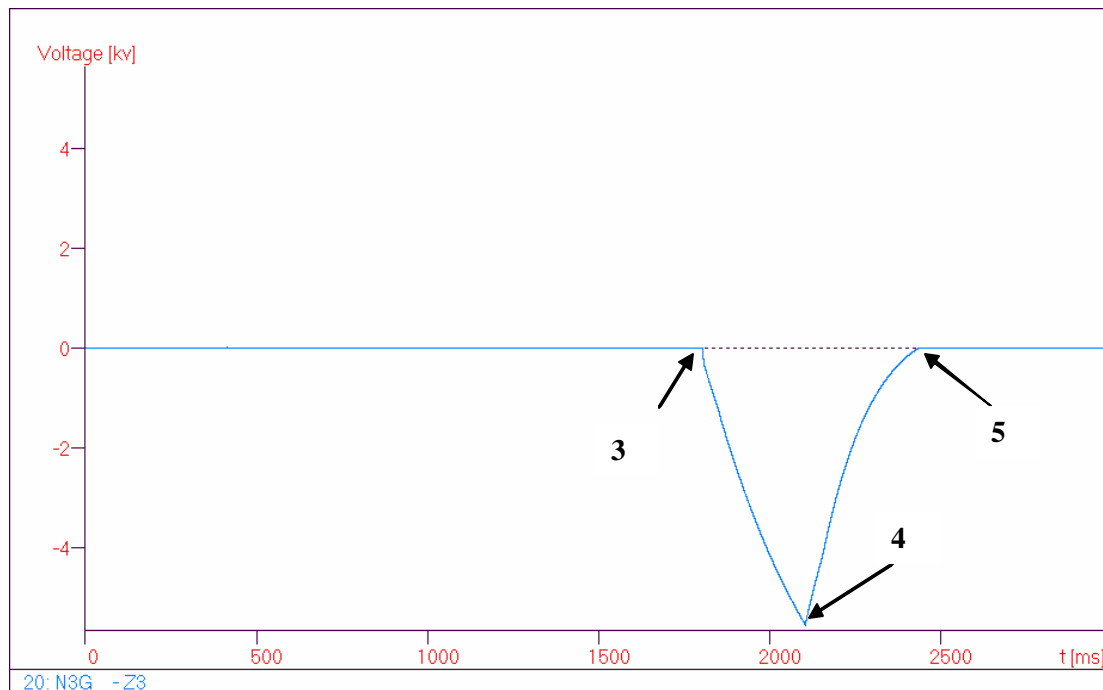


Figure 7.5 Voltage across the left diode on Node N3

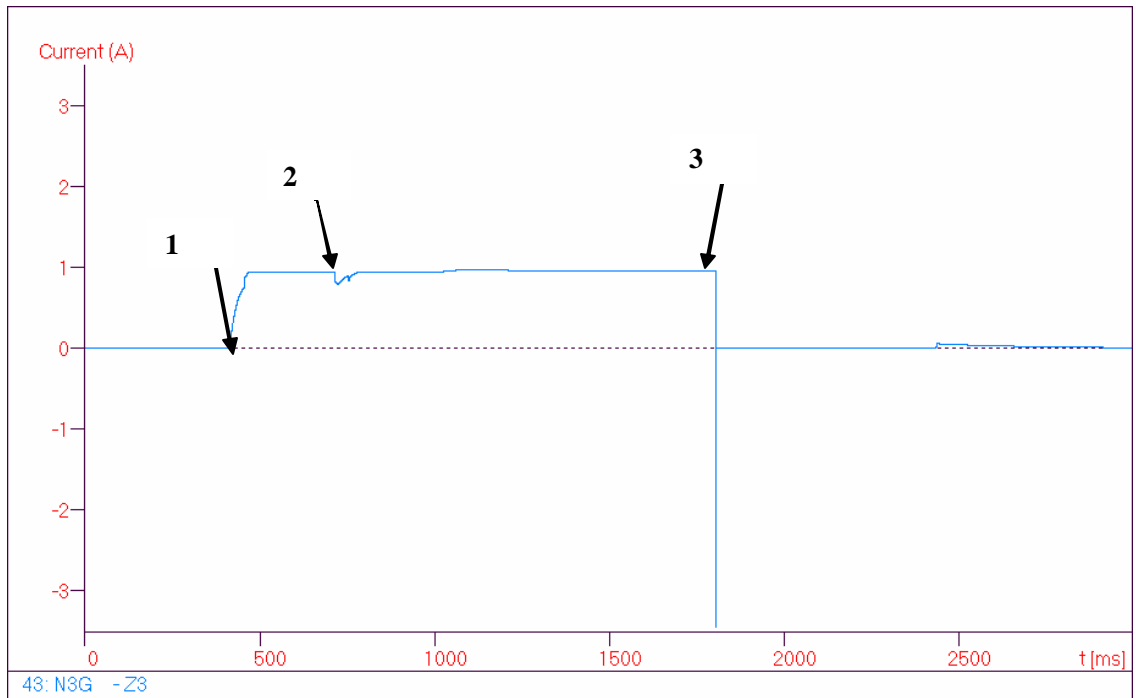


Figure 7.6 Current through the left diode of Node N3

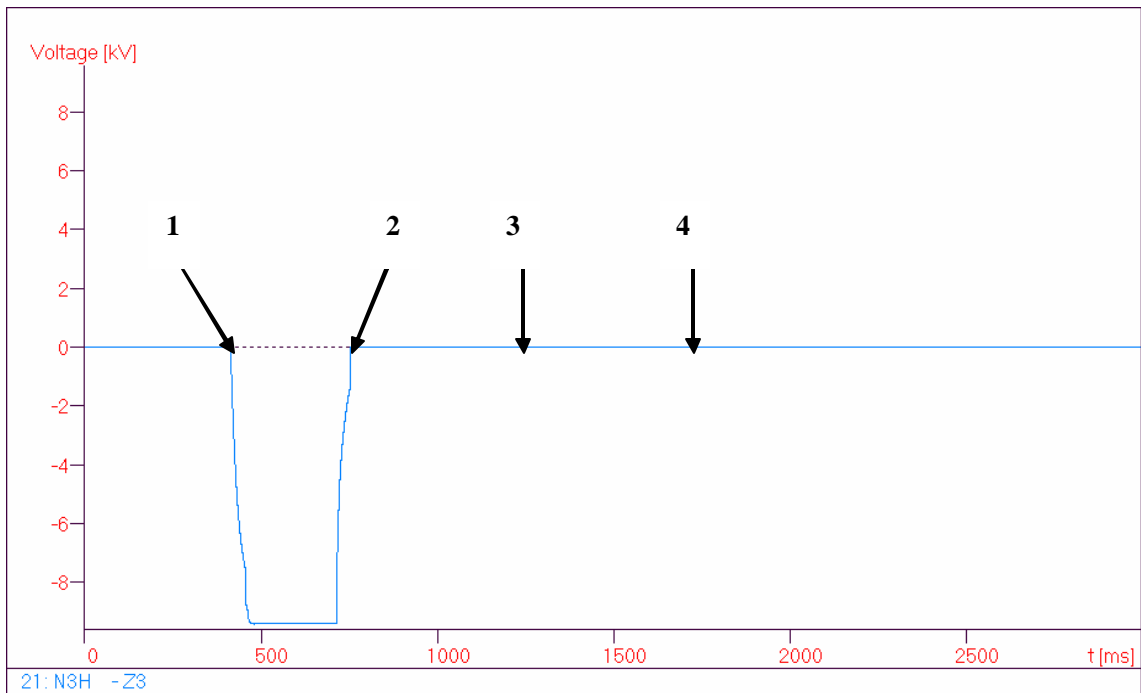


Figure 7.7 Voltage across the right diode of Node N3

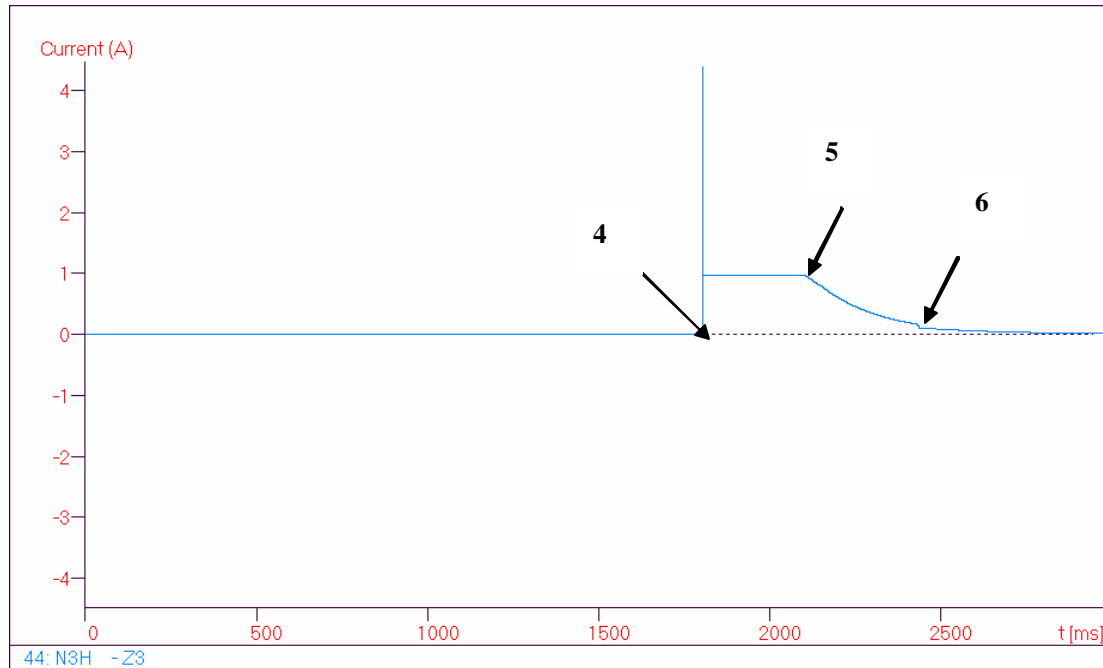


Figure 7.8 Current through right diode of Node N3

Figure 7.7 and Figure 7.8 show the voltage and current of the right diode for Node 3. At 700 ms the breaker of Node 3 closes and hence the voltage across the right diode drops to a minimum because the left diode is conducting and the breaker of Node 3 is closed. At 1.8s the breaker at Node 3 opens and the right diode conducts power fed by shore station V2. At 2.1 s shore station V2 is disconnected when Node 4 opens. The right diode is still forward biased until the capacitance of the cable is fully discharged. The positive current spike seen in Figure 7.8 is the result of numerical error in ATP.

In this simulation, observing the current and voltage waveforms at any given point in the circuit presents an accurate picture of the circuit condition and the status of different components.

7.3 Version 1: Simulation of Fault Condition

In order to understand the dynamics of the NEPTUNE network, it is necessary to simulate the worst-case scenario for current and voltage transients. These transients will be most severe when there is a phase to ground fault. Such a circuit is simulated in Figure 7.9.

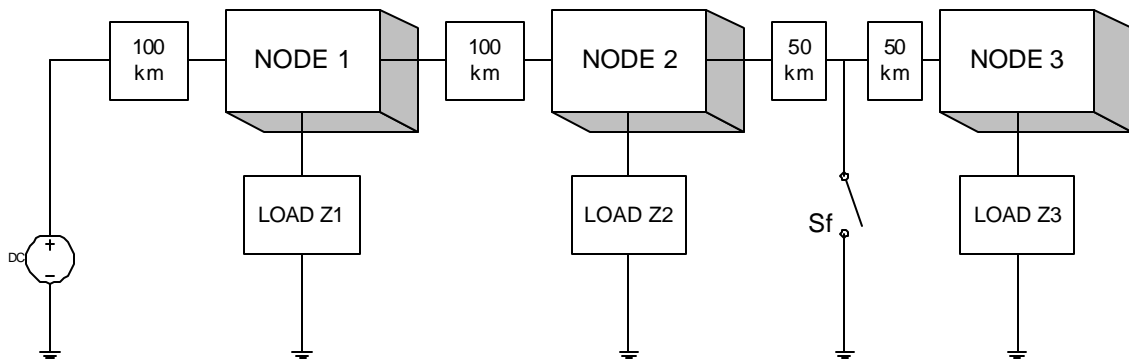


Figure 7.9 Simulation of fault condition

Simulating fault conditions assumes a fault occurring in the middle of the cable between Node 2 and Node 3 at 1.0s. The fault is cleared by initiating the opening sequence of the breaker in Node 2 after 5 ms. When S3 of Node 2 opens, the bypass capacitor starts charging. When the capacitor is fully charged, the fault current is zero and the breaker can be opened fully. The process opening the circuit breaker in Version 1 is explained in Chapter 2.

The occurrence of a fault will cause a current surge of 60A into Node 2 (Figure 7.10). This in turn causes a drop in the input voltage of the node converters (Figure 7.11). It should be noted that no restrikes occur due to the large value of the capacitor. At point 2 the fault is isolated and the voltage starts rising again.

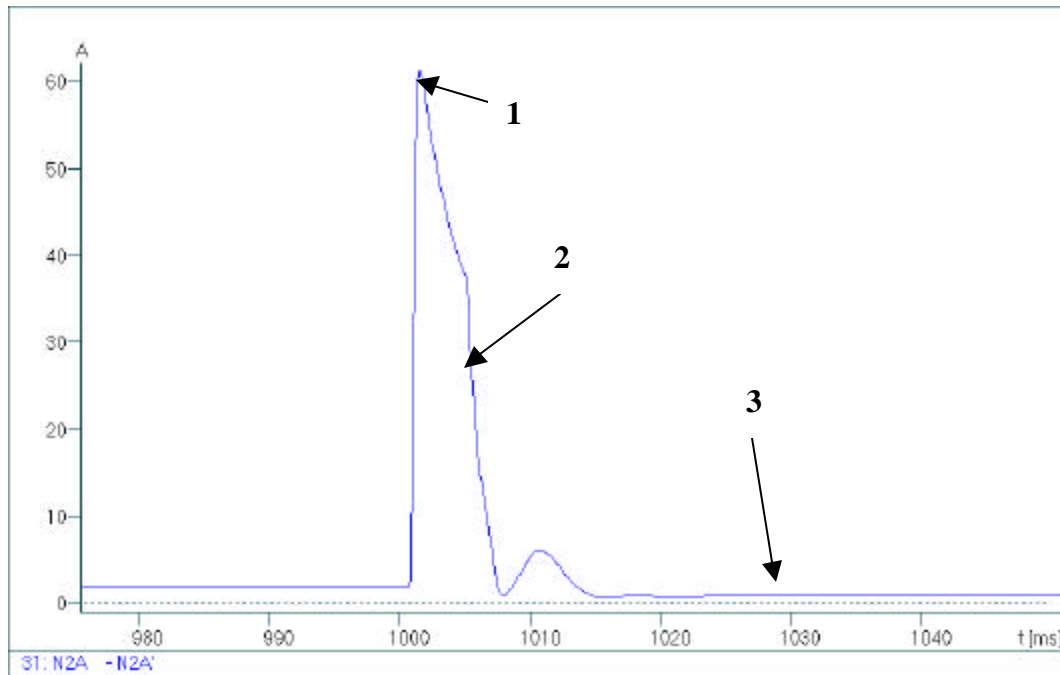


Figure 7.10 Current entering Node 2

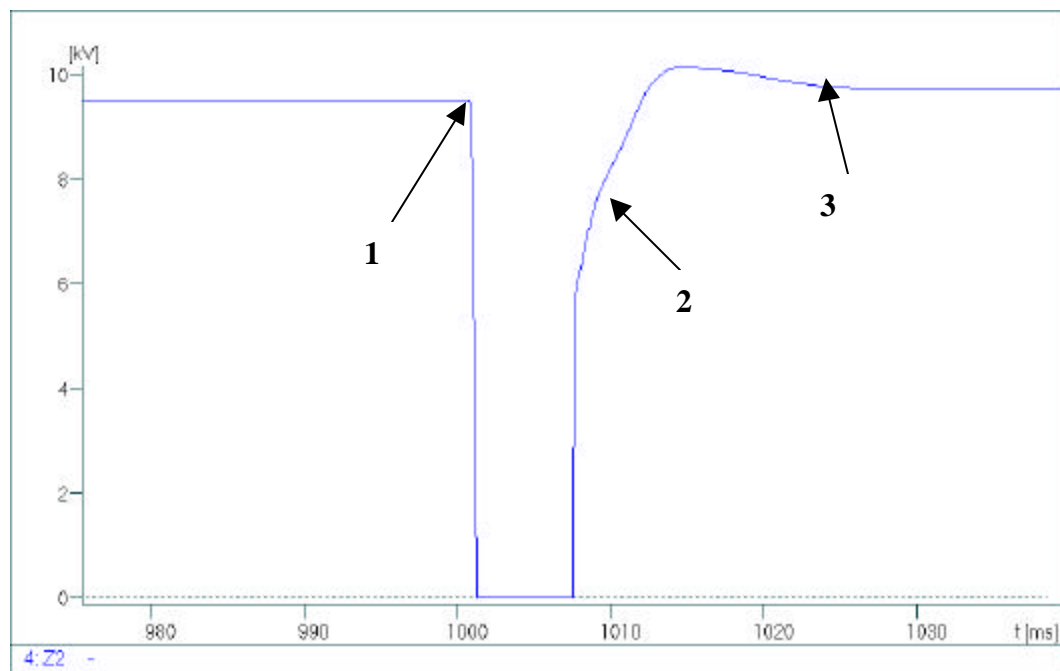


Figure 7.11 Voltage across Load Z2

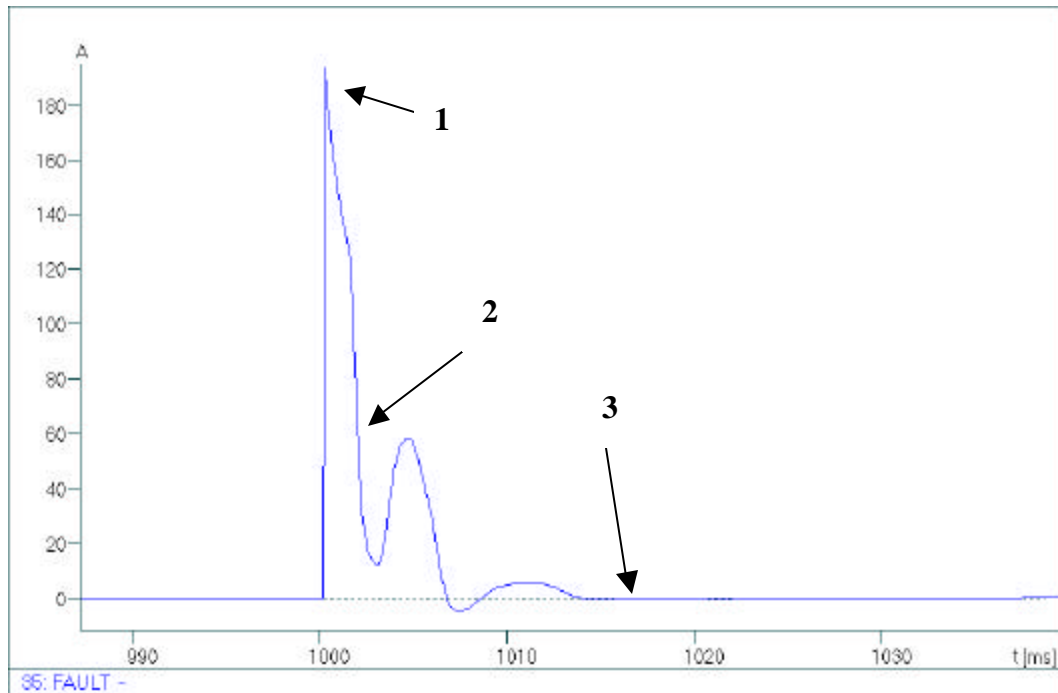


Figure 7.12 Current flowing in fault

Figure 7.12 shows the current flowing through the fault into the ground. Comparing Figure 7.10 and Figure 7.12, it is apparent that the waveforms have a similar shape and hence similar frequency content. However, the magnitude of the transient current into the fault is about 180A, as opposed to the 60A in Node 2. Thus, transients generated at the fault location travel back towards the node, but are suppressed to a large extent by the cable resistance and inductance.

If the fault location is at the node N2, the current into the node N2 will be the same as the current into the fault (Figure 7.12). The current transients experienced by the node electronics are much more severe in this case, thus the node components must be designed to withstand these worst-case transients.

Figure 7.13 shows the current through the capacitor. At the 1.0s mark the fault occurs and 5ms later the node N2 controls react to the fault overcurrent. The switch across the

capacitor is opened and the fault current is diverted through the capacitor causing the capacitor to charge and the current through the capacitor to drop exponentially. At point 2 the circuit breaker is completely opened. At point 3 the capacitor is discharged through a resistor and is then ready for the next cycle of breaker operations.

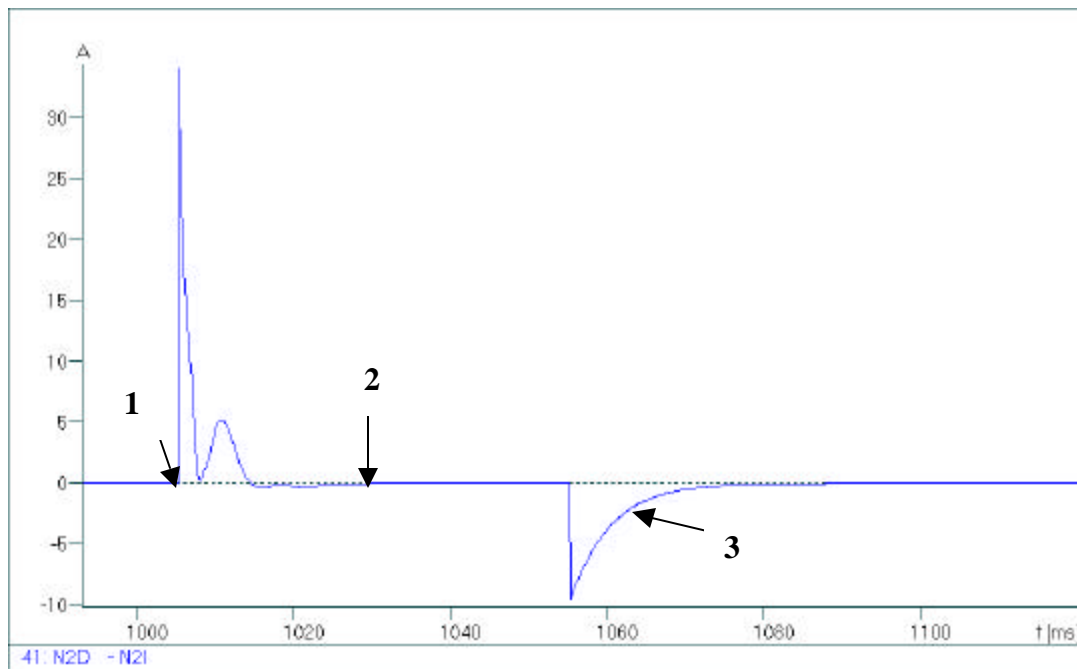


Figure 7.13 Capacitor current for node N2

7.4 Version 2: Fault Transient Studies

In Version 2 the system is re-energized during restoration mode. As explained in Chapter 3, the restoration mode operates at the 5kV level. Thus, during the sequential closing of the circuit breakers in the BUs, the inrush currents are lower than those of Version 1. Further, a current-limiting circuitry at the shore restrains the current to 10A and the transients experienced by the electronics are less damaging.

When a fault occurs, the Version 2 BU responds by going into fault mode. The shore station controls interrupt the power supply. When the system de-energizes, the circuit breakers open. Thus, the circuit breaker in Version 2 never interrupts fault current so it is never subjected to arcing, restrikes, overcurrent, high di/dt and high dv/dt , rendering the complex circuit breaker (Figure 2.4) unnecessary. Instead, the circuit breaker in the BU is implemented as a simple switch. This is one of the main advantages of Version. The fault transient studies for Version 2 are not required for component design but are useful for system analysis.

7.4.1 Placement of pre-insertion resistance in BU

One design consideration of Version 1 is whether a pre-insertion resistance is required in each BU. This resistance is introduced into the circuit by the nearest BU when it sees a fault. Thus, the fault current is immediately reduced and the BU electronics are protected. However, the pre-insertion resistance requires a switch across it. The resistance is introduced into the circuit when the switch is opened, increasing the complexity of the BU. The switch is also opening in the presence of fault current, thereby increasing the possibility of arcing and restrikes.

For faults closer to shore, the shore station enters current-limiting mode and the fault current is reduced almost immediately. The response time of the BU and the shore station controls is almost the same for such faults. For faults further away from the shore, the high cable impedance limits the fault current. This analysis shows that pre-insertion resistance in the BU is unnecessary.

7.4.2 Placement of pre-insertion resistance at the shore station

The pre-insertion resistance may be placed at the shore station. The idea is to insert a resistance of finite value to limit the fault current, before the system enters fault mode and completely shuts down the supply.

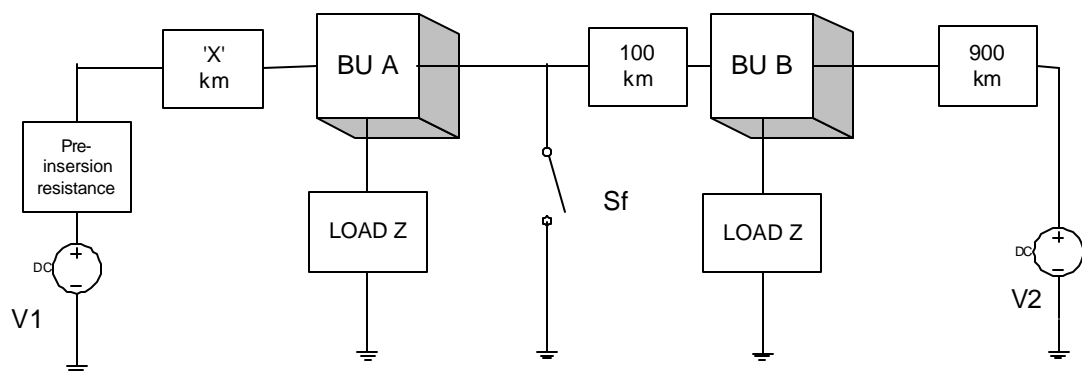


Figure 7.14 Simulation circuit for study of pre-insertion resistance placement

Figure 7.14 shows the simulation circuit for this study. It has two shore stations at both ends rated at 10kV dc. The system is initially assumed to be in the normal mode of operation. The fault is simulated by the switch Sf located at a fixed distance of 1000km from shore station V2. The fault is located to the right of BU A while BU B is 100km from BU A. For this study, the distance between BU A and the shore station V1 is assumed to be 'X' km. The value of X is varied for different sets of simulations.

There are three controllable parameters in the simulations:

1. Value of the pre-insertion resistance at the shore station V1
2. Response time of the shore station control circuitry to insert resistance
3. Distance of the fault from shore station V1

Simulations are performed for three different sets. In each set, one of the above parameters is varied while the others remain constant. The quantities measured are the peak transient current at the fault location and the I^2t value of the fault. The I^2t value gives an indication of the amount of energy dumped into the fault during a certain transient time. For this study, a transient time of 100ms is assumed.

7.4.2.1 Simulation set A

For this simulation set, the response time of the shore station circuitry is kept constant at 15ms. This value includes the time to open the switch across the pre-insertion resistor. The distance of shore station V1 from the fault, X, is kept constant at 100km. Thus, the fault is close to the shore. The pre-insertion resistance is varied. The peak transient current and the I^2t value are measured. It is found that for any value of pre-insertion resistance, the peak transient current is constant at 176A and the I^2t value is constant at 175.

The same simulation is carried out again, with the location of fault at 1200km from shore station V1. In this case, the fault is far away from the shore. Again, the peak transient current and the I^2t value are constant for different pre-insertion resistance values, but the constant peak transient current is 56A and the constant I^2t value is 13.5.

This simulation shows that the shore station controls cannot react fast enough to affect the peak current transient or the fault energy. The peak values are dependent on the amount of energy stored in the cable capacitance and the fault location.

7.4.2.2 Simulation set B

In this simulation set, the response time of the shore station circuitry is varied. The response time includes the time to open the switch across the pre-insertion resistor. The distance of shore station V1 from the fault, X, is kept constant at 100km. In another

simulation, the value of X is changed to 1200km. The value of the pre-insertion resistor is kept constant at $100\text{k}\Omega$ for both simulations. Again, the peak transient current and the I^2t are measured.

Both simulations show that the peak transient current remains constant and is independent of the shore station response time. The peak transient current is 176A and 56A for the 100km and 1200km fault distances, respectively. The I^2t value varies with the simulated response time of the shore station (Figure 7.15).

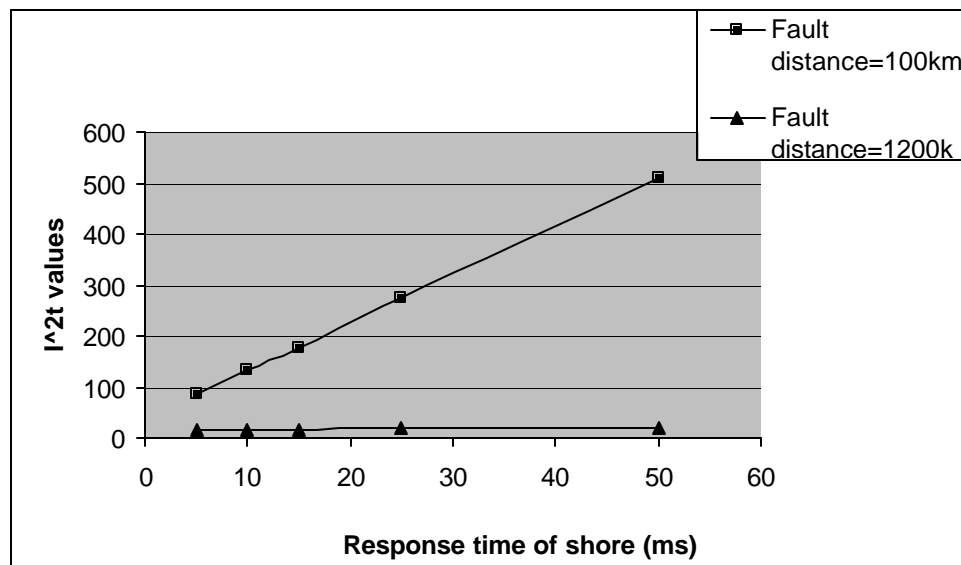


Figure 7.15 Plot of fault energy against response time

7.4.2.3 Simulation set C

In these simulations, the pre-insertion resistance is kept constant at $100\text{k}\Omega$ and the shore station response time is constant at 15ms. The fault distance, X , is varied from 50km to 1000km. Here, the simulated peak transient currents, as well as the fault energy represented by the I^2t value vary with the fault location (Figure 7.16 and Figure 7.17).

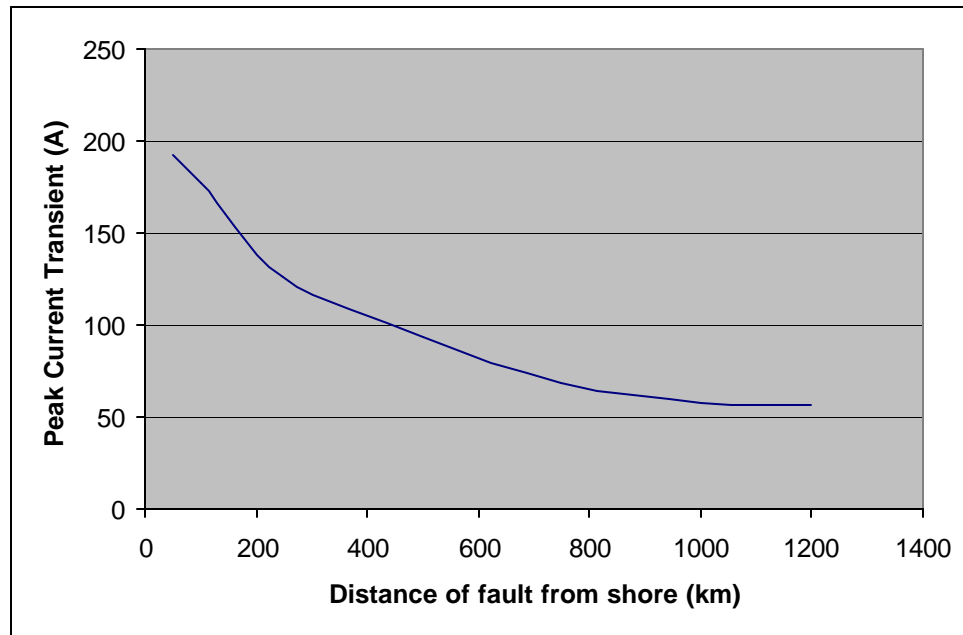


Figure 7.16 Plot of peak transient current against the fault distance 'X'

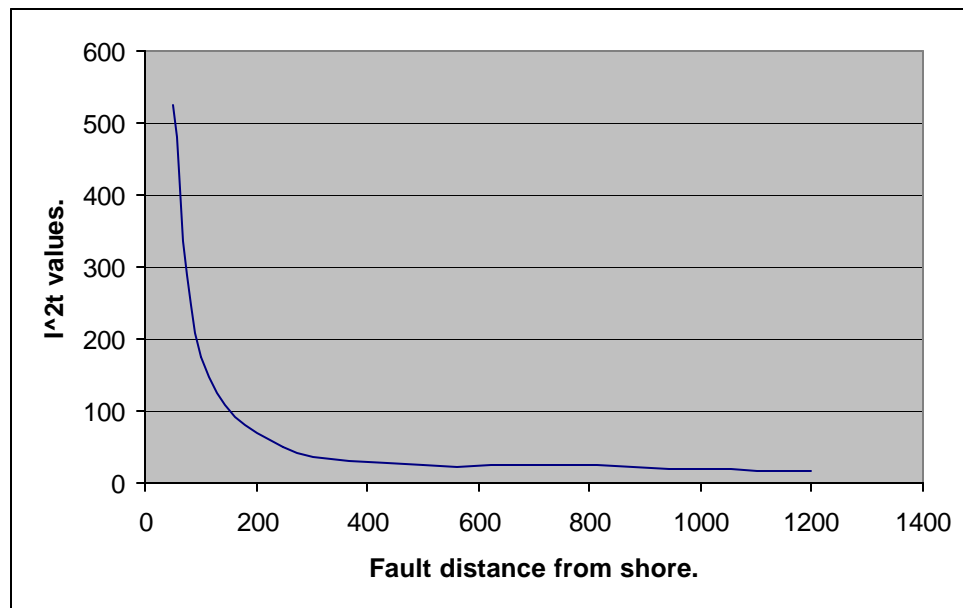


Figure 7.17 Plot of fault energy against the fault distance 'X'

The simulations show that there is no significant advantage in placing a pre-insertion resistor at the shore station. The pre-insertion resistor does not affect the peak transient current at the fault location or the fault energy. The shore station current-limiting circuitry is fast enough to quickly restrain the fault current.

Chapter 8. Conclusions and Future Work

The aim of NEPTUNE is to design an underwater observatory that will be a base for scientific research in the sub-sea environment. Currently, the geographical reach of such an observatory is limited to the Juan de Fuca plate on the Pacific coast. The aim is to further expand the size of the network and make more ocean area available for scientific research.

The power system design of NEPTUNE presents many challenges. An undersea, 10kV dc network has no parallel in the world of conventional terrestrial power systems. The power delivery system includes a standard telecom cable, from which power is tapped at fixed locations or nodes. The node dc-dc converter steps down the 10kV backbone voltage to 400V, which will be used by the end-science users.

The Version 1 power system is designed along the lines of a conventional power system. The Protection, Monitoring and Control System (PMACS) of Version 1 is similar to the SCADA (Supervisory Control and Data Acquisition) system. In response to a fault, the Version 1 controller trips the nearest circuit breaker. A complicated circuit breaker is designed to interrupt the dc fault current. Version 1 is likely to be unreliable as it depends largely on the node dc-dc converter. A single failure in the node converter can render a large part of the system unoperational. Because, maintenance of the NEPTUNE power system is both complicated and costly, it is necessary to make most of the control actions autonomous and highly reliable. This is a difficult goal to achieve using Version 1. Further, studies indicated that a fault in the Version 1 power system would cause a voltage collapse in a large number of nodes, making the process of fault isolation difficult to achieve.

The Version 2 power system is based on the presumption that faults in underwater power cables are very rare. The response to a fault is drastic, as the entire system shuts down. This is followed by a process whereby the fault is located and the system is restored.

Because a node failure (failure of the node converter for example) will not render the system unoperational, Version 2 is more reliable. The cost of the Version 2 power system is lower due to reduced node and BU complexity. Also, the high-cost, two-conductor spur cable between the branching units and nodes in Version 1 is no longer required.

The transient analyses for Version 1 were done using the ATP-EMTP software. Different worst-case scenarios were simulated for system component design and failure analysis. Restrike and shore station control models are developed and used in these simulations. One of the most important factors for the accuracy of the simulations is the cable model. In this work, results from a theoretical study of the NEPTUNE cable were compared with the data provided by the cable manufacturer and with the ATP simulation results.

Future Work

Version 2 is the preferred design for the NEPTUNE power system. The dc circuit breaker prototype for Version 2 and its control and monitoring systems will be constructed. This includes the design of the BU controller using microcontroller or array logic. This work involves the development of both a lab prototype as well as a 10kV high voltage prototype.

A complete transient model must be created for the entire NEPTUNE system. Such a model must be generic and have the capacity to simulate any type of fault condition for any operating scenario. Such a model will eventually be a part of the software package that will be used in the day-to-day operation of the NEPTUNE power system.

List of References

- [1] NEPTUNE Feasibility Study, “Real Time, Long Term Ocean and Earth Studies at the Scale of a Tectonic Plate”, available at the website www.neptune.washington.edu
- [2] B.M.Howe, H.Kirkham, V. Vorperian, “Power system considerations for undersea observatories,” *IEEE Journal of Ocean Engineering*, Vol.27, No.2, April 2002.
- [3] Website, “www.emtp.org”.
- [4] B.M.Howe, H.Kirkham, V.Vorperian, “Power system considerations for undersea observatories,” *IEEE Journal of Oceanic Engineering*, Vol27, No.2 April 2002.
- [5] A.Upadhye, M.A.El-Sharkawi, “Node-Backbone DC Switchgear Concept,” NEPTUNE Power Concept Design Review, June 2002. Website ‘<http://neptunepower.apl.washington.edu/documentation/documentation.html>’.
- [6] Jian Xing, “Adaptive Sequential Controller and A Timing Control Scheme for Solid State Power Switching in Floating Neutral Systems,” Ph.D. Thesis, University of Washington, 1996.
- [7] “Circuit Interruption, Theory and Techniques,” Edited by Thomas E. Browne Jr., Published by Marcel Dekker, Inc.
- [8] Lou van der Sluis, “Transients in Power Systems,” Published by John Wiley & Sons, Ltd.
- [9] H.W.Dommel, W. S. Meyer, “Computation of Electromagnetic Transients,” *Proceedings of the IEEE*, Vol. 62, No. 7, July 1974.
- [10] EMTP Theory Book, Canadian/American EMTP User Group, 1987-2000 (distributed by EEUG).

- [11] K.Strunz, "Computer aided analysis and simulation of electric circuits and networks," lecture notes.
- [12] Meyer, W.S.; Liu, T.-H, "Alternative Transients Program (ATP) Rule Book," Canadian/American EMTP User Group, 1987-2000 (distributed by EEUG).
- [13] Prikler, L.; Hoidalen H.K., "ATPDraw User's Manual," 1998 (distributed by EEUG).
- [14] Marti, J.R., "Accurate Modeling of frequency-dependant transmission lines in electromagnetic transient simulations," *IEEE Transactions on PAS*, Vol. PAS 101, No.1, pp147-155, Jan 1982.
- [15] Bode H.W., "Network Analysis and Feedback Amplifier Design" New York: Van Nostrand, 1945.
- [16] "Handbook of mathematical functions," edited by M.Abramowitz and I.A.Stegun, publ. By US Dept. of Commerce, 1964.
- [17] Bianchi, G. and Luoni, G., "Induced Currents and Losses in Single-core Submarine Cables," *IEEE Transactions on PAS*, Vol.- PAS-95, no.1, January/February 1976.